History-Dependent Physiological Adaptation to Lethal Genetic Modification under Antibiotic Exposure

Yuta Koganezawa[1], Miki Umetani[1,2], Moritoshi Sato[2-4], Yuichi Wakamoto[1,2,4,*]

1 Department of Basic Science, Graduate School of Arts and Sciences, The University of Tokyo
2 Research Center for Complex Systems Biology, The University of Tokyo
3 Department of Life Sciences, Graduate School of Arts and Sciences, The University of Tokyo
4 Universal Biology Institute, The University of Tokyo

* cwaka@mail.ecc.u-tokyo.ac.jp

Abstract

Genetic modifications, such as gene deletion and mutations, could lead to significant changes in physiological states or even cell death. Bacterial cells can adapt to diverse external stresses, such as antibiotic exposure, but can they also adapt to detrimental genetic modification? To address this issue, we visualized the response of individual *Escherichia coli* cells to deletion of the antibiotic resistance gene under chloramphenicol (Cp) exposure, combining the light-inducible genetic recombination and microfluidic long-term single-cell tracking. We found that a significant fraction (∼40%) of resistance-gene-deleted cells demonstrated a gradual restoration of growth and stably proliferated under continuous Cp exposure without additional mutations. Such physiological adaptation to genetic modification was not observed when the deletion was introduced in 10 h or more advance before Cp exposure. Resistance gene deletion under Cp exposure disrupted the stoichiometric balance of ribosomal large and small subunit proteins (RplS and RpsB). However, the balance was gradually recovered in the cell lineages with restored growth. These results demonstrate that bacterial cells can adapt even to lethal genetic modifications by plastically gaining physiological resistance. However, the access to the resistance states is limited by the environmental histories and the timings of genetic modification.

Introduction

Bacteria in nature are constantly challenged by environmental and genetic perturbations and must be robust against them for survival. Bacterial cells possess programs to adapt or resist such perturbations. For example, under the conditions of nutrient deprivation, *E. coli* and related bacteria provoke RpoS-mediated general stress response and globally change the metabolic and gene expression profiles to protect themselves from the stress [1]. DNA damage also induces SOS response, which promotes both DNA repair and mutagenesis [2,3]. If the mutations in essential genetic elements remain unrepaired, their influence will be propagated to cellular phenotypes or even cause cell death. How rapidly new genetic changes alter cellular phenotypes and whether they always give rise to the same phenotypes in given environments are fundamental questions in genetics [4,5]. Nevertheless, such time-dependent and redundant genotype-phenotype correspondences are usually deemed negligible or insignificant in most genetics analyses.

However, the evidence suggests that biological systems can buffer or compensate for the impact of genetic changes at the cytoplasmic and physiological levels [6]. For example, specific molecular chaperons could hinder genetic variations from manifesting as morphological and growth phenotypes in fruit flies [7],

plants [8], and bacteria [9]. Furthermore, the loss of biological functions caused by genetic changes can be compensated for by modulating the RNA and protein levels of the mutated or other related genes in many organisms [10]. In *Bacillus subtilis*, the expression noise of mutant sporulation regulator results in the partial penetrance of its influence to spore-forming phenotypes [11]. These observations across diverse organisms suggest that phenotypic consequences of genetic modifications can be modulated based on environmental and physiological contexts, which may promote the survival and evolution of the organisms.

Despite these experimental implications, it remains elusive whether bacterial cells can circumvent even lethal genetic modifications such as antibiotic resistance gene deletion under antibiotic exposure. Furthermore, how cells initially respond to the genetic changes and how their physiological and phenotypic states are modulated in longer timescales are poorly characterized. However, addressing these issues requires precisely defining the timings of genetic changes and tracking individual cells for a long period to unravel their phenotypic transitions and consequences [5].

In this study, we resolve these technical issues by combining the photoactivatable Cre (PA-Cre) light-inducible genetic recombination technique [12] and microfluidic long-term single-cell tracking [13]. We induced a pre-designed deletion of chromosomally-encoded and fluorescently-tagged drug resistance gene in *E. coli* directly in the microfluidic device. The results show that all of the resistance-gene-deleted cells under continuous drug exposure showed a decline in growth in 5-7 generations, but a fraction of the resistance-gene-deleted cells gradually restored their growth without additional mutations. In contrast, no cells restored growth when the same deletion was introduced 10 h or more in advance before drug exposure. Therefore, bacterial cells can physiologically adapt to lethal genetic modifications. However, its feasibility depends on environmental histories and the timings of genetic modifications.

Results

Resistance gene deletion in *E. coli* by blue-light illumination

To investigate the response of individual cells to antibiotic resistance gene deletion, we constructed an *E. coli* strain expressing chloramphenicol acetyltransferase (CAT) tagged with mCherry red fluorescent protein (Fig. 1A). CAT confers resistance to chloramphenicol (Cp) by acetylating Cp [14]. The *mcherry-cat* resistance gene was integrated on the chromosome along with the upstream and downstream *loxP* sequences so that the resistance gene could be excised by Cre recombinase (Fig. 1A). We also introduced the PA-Cre recombination system, which consists of split Cre-recombinase fragments, called CreC and CreN, attached to p-Magnet (p-Mag) and n-Magnet (n-Mag) monomers, respectively (Fig. 1B) [15]. p-Mag and n-Mag are heterodimers derived from the fungal photo-receptor, Vivid [15], which heterodimerize upon blue-light illumination. In the PA-Cre system, blue-light illumination leads to heterodimerizations of p-Mag-CreC and n-Mag-CreN fragments and recovers Cre recombination activity (Fig. 1B) [12]. Therefore, this system allows us to induce the resistance gene deletion at arbitrary timings by blue-light illumination. The original PA-Cre system was designed for use in mammalian cells [12]; we thus replaced the plasmid backbone and the promoter for use in *E. coli*.

We first analyzed the response of the constructed strain YK0083 to blue-light illumination under drug-free conditions. Single-cell observations with the mother machine microfluidic device [13] and custom stage-top LED illuminator (Fig. S1) revealed that 30-min blue-light exposure (λ =464∼474 nm, 6.8 mW at the specimen position) led to the loss of mCherry-CAT fluorescence in 25% (50/200) cells (Fig. 1C, D, and Movie S1), suggesting the deletion of the *mcherry-cat* gene in these cell lineages. The fluorescence signals decayed to the background level in 4-5 generations, and the decay kinetics was consistent with the dilution by growth (Fig. 1D). Furthermore, the 30-min blue-light illumination and genetic recombination did not affect the growth of individual cells (Fig. 1E).

Extending illumination duration increased the frequency of cells showing loss of fluorescence, reaching 100% ($n = 296$) in 4 h (Fig. S2A and B). We confirmed the correspondence between the loss of mCherry fluorescence and *cat* gene deletion by colony PCR (Fig. S2C).
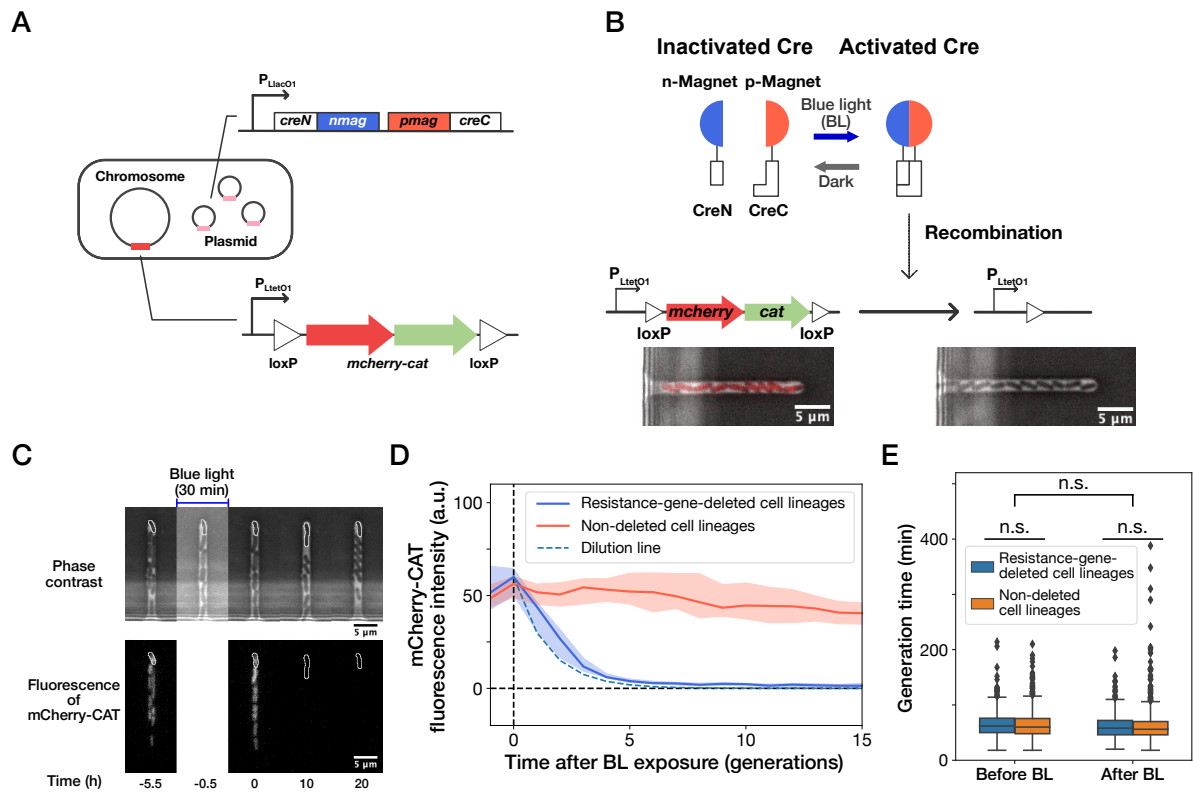
Figure 1. Live-cell monitoring of phenotypic transitions in response to gene deletion. (A) Schematic drawing of an *E. coli* strain, YK0083. This strain harbors the photo-removable *mcherry-cat* gene on the chromosome and a low-copy plasmid carrying the pa-cre genes (*creN-nmag* and *pmag-creC*). (B) The PA-Cre system. Blue-light illumination provokes the dimerization of two PA-Cre fragments and induces the deletion of the *mcherry-cat* gene. The micrographs represent the combined images of phase contrast and mCherry-CAT fluorescence channels. Left and right images show the cells before and after blue-light illumination, respectively. (C) Representative time-lapse images of gene-deletion experiments. The upper and lower images show the cells in phase contrast and mCherry-CAT fluorescence channels, respectively. The cell lineages at the closed end of the growth channel (outlined in white) were monitored. A 30-min blue-light illumination starting at $t = -0.5$ h led to the loss of mCherry-CAT fluorescence signals in this cell lineage. (D) The transitions of mCherry-CAT fluorescence intensities in resistance-gene-deleted (blue) and non-deleted (red) cell lineages. Lines and shaded areas represent the medians and the 25-75% ranges, respectively. The cyan broken line represents the expected fluorescence decay curve when the fluorescence intensity decreases to half in each generation. (E) Generation time of resistance-gene-deleted and non-deleted cells ten generations before and after blue-light illumination. The middle line and both edges of the boxes represent the medians and the 25-75% ranges of generation time. Whiskers indicate the minimum and maximum of the data except for the outliers. The points represent the outliers. No significant differences in generation time were detected between the groups at the significance level of 0.01 ($p = 0.47$ for before BL, $p = 0.027$ for after BL, $p = 0.084$ for before BL vs after BL, Mann-Whitney U test).

Fractional continuation of growth against resistance gene deletion under drug exposure

We next induced the deletion of the resistance gene in YK0083 cells in the mother machine, continuously flowing a medium containing 15 μg/ml of Cp. This drug concentration was 1.5-fold higher than the minimum inhibitory concentration (MIC) of the non-resistant strain YK0085 (10 μg/ml), which was constructed by illuminating the YK0083 cells by blue light in batch culture (Fig. S3). Therefore, it was expected that this drug concentration would inhibit the growth of resistance-gene-deleted cells. This Cp concentration was significantly lower than the MIC of resistant YK0083 cells (100 μg/ml, Fig. S3) and did not influence their growth rates (Fig. S4).

A 30-min blue-light illumination induced the *mcherry-cat* gene deletion in 24.5% (343/1399) in YK0083 cells (Fig. 2A and Movie S2). While non-deleted cells continued to grow with their generation time (interdivision time) and mCherry-CAT fluorescence intensity nearly unaffected (Fig. 2B and C), resistance-gene-deleted cells gradually showed a decline in growth (Fig. 2D-G). The fluorescence intensity of the resistance-gene-deleted cells decayed to the background levels in 4-5 generations (Fig. 2D, F, and H), and their generation time also increased correspondingly (Fig. 2E, G, and I). However, while the growth of 62.7% (163/260) of resistance-gene-deleted cells was eventually stopped, the other 37.3% cells restored and continued their growth over 30 generations without the *cat* resistance gene (Fig. 2H and I). The generation time of these cell lineages recovered from 6.3 h (the median of 6th-9th generations) to 3.0 h (the median of 21st-30th generations) under the continuous drug exposure (Fig. 2I). The elongation rate transitions across multiple generations also manifested the growth recovery (Fig. S5).

We first suspected that the growth recovery under Cp exposure was attributed to the presence of the *cat* gene untagged from the *mcherry* gene or by additional unintended resistance-enhancing mutations. To test this hypothesis, we sampled the culture media flowing out from the microfluidic device and obtained cell populations derived from a single or few ancestral cells by limiting dilution (Fig. S6A). PCR analysis confirmed the lack of *cat* gene in the non-fluorescent cell populations (Fig. S6B). Furthermore, whole-genome sequencing of the cell populations obtained by limiting dilution showed no additional mutations in 4 out of 5 non-fluorescent cell populations tested (Table S1). One point mutation was present in one cellular population, but this mutation did not affect the MIC (Fig. S6C). Therefore, it was unlikely that unintended genetic changes were responsible for the growth restoration. It is also unlikely that the growth restoration was caused by the residual mCherry-CAT proteins because 30 consecutive cell divisions dilute cytoplasmic proteins $2^{30} \approx 10^9$ folds if additional production is prevented; note that even the total number of protein molecules in a bacterial cell are in the order of 10^6-10^7 [16];

We also detected no significant differences in the mCherry-CAT fluorescence intensity before blue-light illumination between the growth-halted and growth-restored cell lineages (Fig. S7A). Furthermore, no significant differences were observed even between the resistance-gene-deleted and non-deleted cell lineages (Fig. S7A). We also examined the influence of elongation rate before blue-light illumination on the gene deletion and the fates after gene deletion, finding no correlations (Fig. S7B). Therefore, neither the amount of mCherry-CAT proteins at the time of gene deletion nor pre-deletion elongation rate affected the likelihood of gene deletion and the determination of growth-halt and growth-restoration fates under these experimental conditions.

Resistance gene deletion long before Cp exposure prevents growth restoration

The high frequency of growth restoration observed against the resistance gene deletion was unexpected since the MIC of the susceptible strain was below 15 μg/ml (Fig. S3 and S6C). To understand this discrepancy, we cultured the susceptible YK0085 cells in the mother machine first without Cp and then exposed them to 15 μg/ml of Cp directly in the device. In contrast to the previous observation, all cells stopped growth and division entirely, with no cells restoring growth ("Pre-deleted" in Fig. 3A-C and Movie S3). This result excludes the hypothesis that the unique cultivation environments in the microfluidics device are the cause of growth restoration. Instead, this observation implies that the timing of gene deletion is crucial for the cells to withstand the Cp exposure without the resistance gene and restore growth.

To further investigate the importance of the timing of gene deletion, we performed microfluidic single-cell
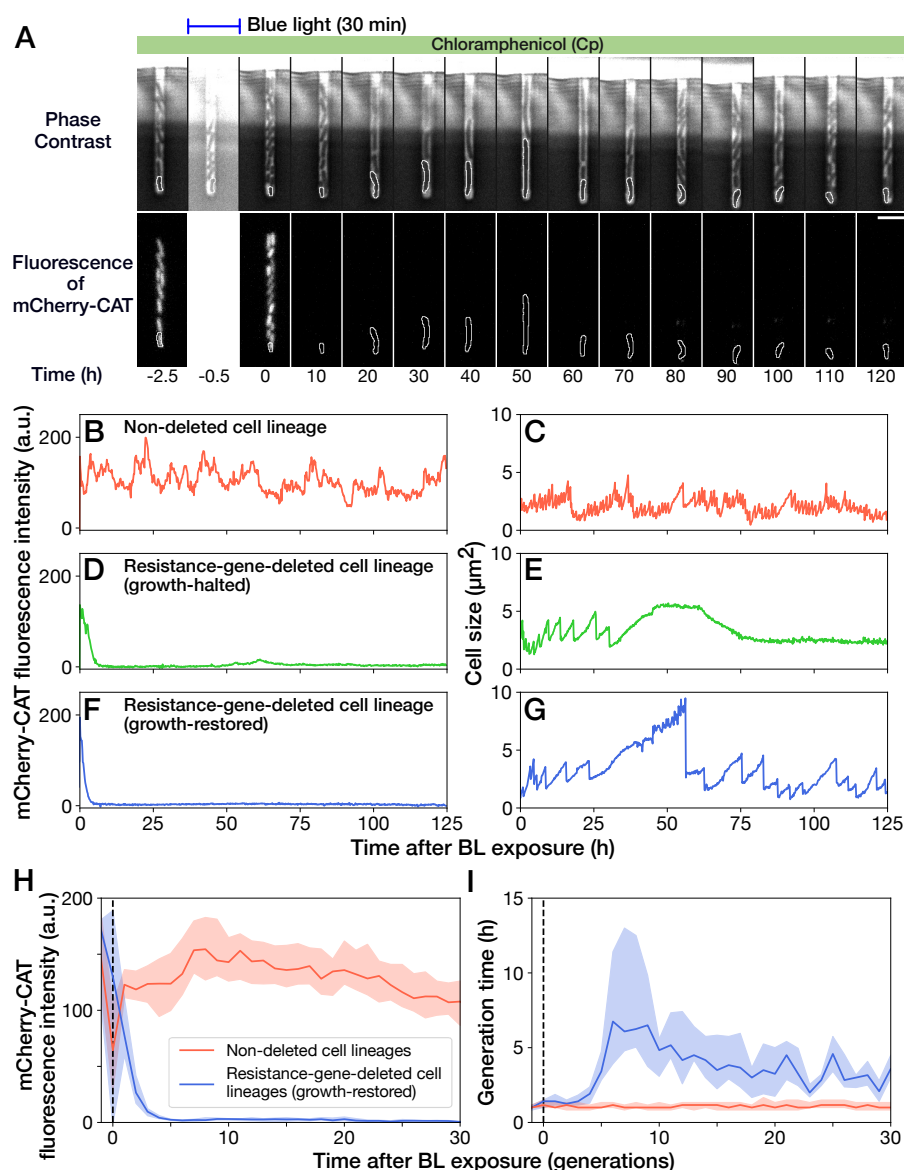
Figure 2. Growth continuation under Cp exposure against *cat* gene deletion. (A) Time-lapse images of a cell lineage that continued growth and division against *mcherry-cat* gene deletion. The upper and lower sequences show phase contrast and mCherry fluorescence images, respectively. Blue light was illuminated from t = -0.5 h to 0 h. The cells at the closed end of the growth channel were monitored during the experiment, which are outlined in white on the images. Scale bar, 5 μm. (B-G) The transitions of mCherry-CAT fluorescence intensities and cell size in single-cell lineages. (B, C) Non-deleted cell lineage. (D, E) Growth-halted resistance-gene-deleted cell lineage. The decrease in cell size after 60 h was due to the shrinkage of the cell body. (F, G) Growth-restored resistance-gene-deleted cell lineage. (H, I) The transitions of mCherry-CAT fluorescence intensities (H) and generation time (I). The lines and shaded areas represent the medians and the 25-75% ranges, respectively. Red represents non-deleted cell lineages. Blue represents growth-restored resistance-gene-deleted cell lineages. The transitions are shown in generations.
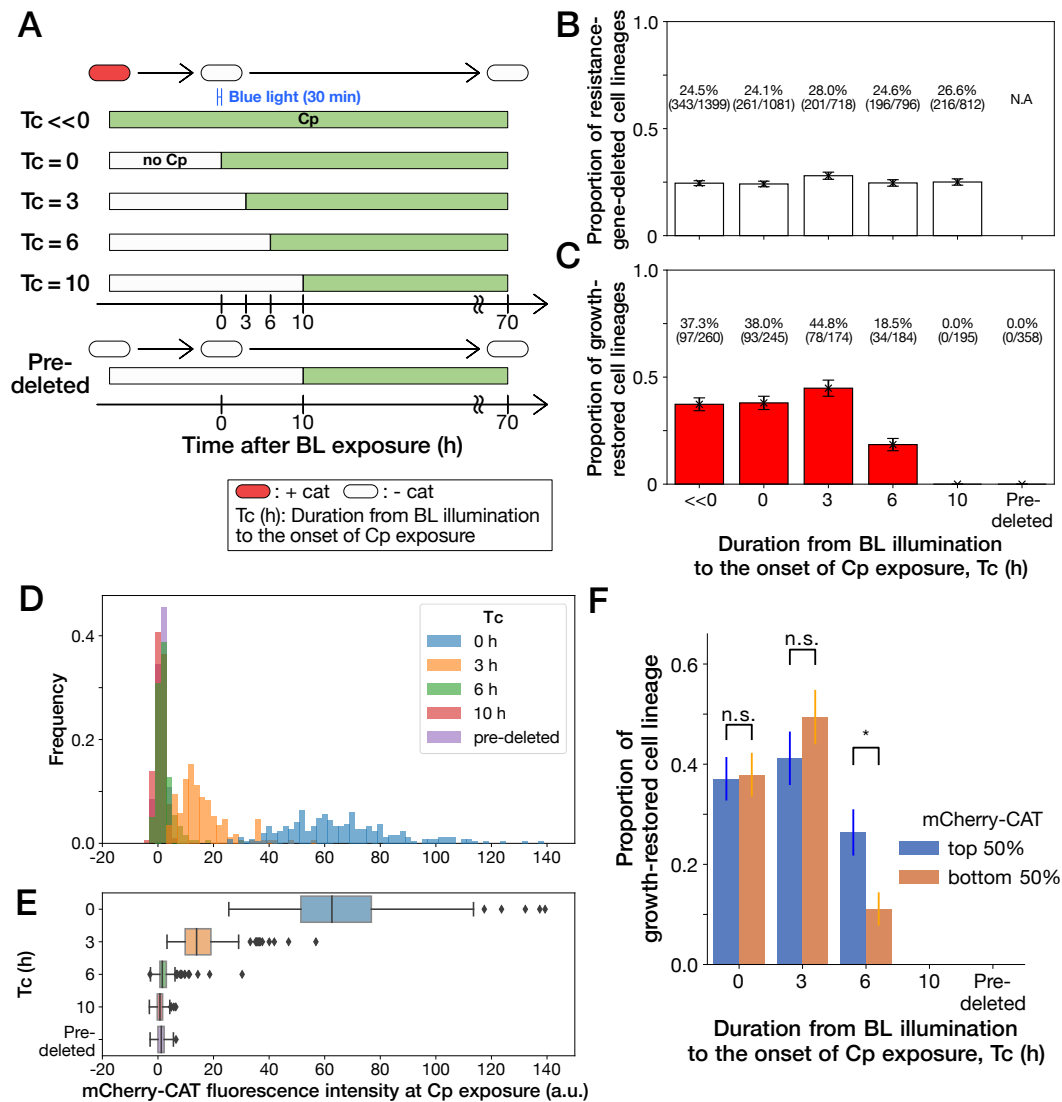
Figure 3. History-dependent maintenance of Cp resistance. (A) The schematic diagram of experiments. The duration from the end of blue-light illumination to the onset of Cp exposure (T_c) was varied from 0 to 10 h. $T_c \ll 0$ represents the continuous Cp-exposure condition. "Pre-deleted" denotes the results of the experiments performed with the *mcherry-cat*-deleted YK0085 strain. The non-resistant YK0085 cells were not exposed to blue light. (B) Fractions of *mcherry-cat*-deleted cell lineages across different T_c conditions. The numbers of resistance-gene-deleted cell lineages among the total numbers of cell lineages observed during the measurements are shown above the bars. Error bars represent standard errors. (C) Fractions of growth-restored cell lineages among resistance-gene-deleted cell lineages. The numbers of growth-restored cell lineages among all the resistance-gene-deleted cell lineages are shown above the bars. Error bars represent standard errors. The numbers of resistance-gene-deleted cell lineages are different from those in B because some cell lineages were flushed away from the growth channels at the later time points of the measurements, and their fates could not be determined. (D, E) The distributions of the mCherry-CAT fluorescence intensities at the onset of Cp exposure across the different T_c conditions represented by histograms (D) and box plots (E). (F) Fractions of growth-restored cell lineages and their dependence on the mCherry-CAT fluorescence at the onset of Cp exposure. Blue and orange bars indicate the fractions of growth-restored cells among cell lineages whose mCherry-CAT fluorescence intensities were higher and lower than the median, respectively. Error bars represent standard errors. The growth-restored cell lineages were not detected under the $T_c = 10$ h and "Pre-deleted" conditions. Fractional differences between the top 50% and the bottom 50% of cell lineages were statistically significant only for the $T_c = 6$ h condition ($p = 0.90$ for $T_c = 0$ h; $p = 0.28$ for $T_c = 3$ h; and $p = 8.6 \times 10^{-3}$ for $T_c = 6$ h, two proportional z-test).

measurements with the resistant YK0083 strain, varying the duration from blue-light illumination to the $_{112}$ onset of Cp exposure (T_c) between 0 h to 10 h (Fig. 3A). The proportions of cells that lost the *mcherry-cat* $_{113}$ gene in response to blue-light illumination almost remained unchanged among all conditions, ranging from $_{114}$ 24-28% (Fig. 3B). However, the proportions of growth-restored cell lineages among resistance-gene-deleted $_{115}$ cells strongly depended on T_c (Fig. 3C). When Cp exposure was initiated immediately after the blue-light $_{116}$ illumination ($T_c = 0$ h) or after 3 h ($T_c = 3$ h), the proportions of growth-restored cells were nearly $_{117}$ equivalent to those observed under continuous Cp exposure conditions (Fig. 3C). In contrast, the proportions $_{118}$ of growth-restored cells were reduced to 18.5% (34/184) when $T_c = 6$ h, and we did not detect any growth $_{119}$ restoration when $T_c = 10$ h (0/195; Fig. 3C). The almost equivalent frequencies of growth-restored cell $_{120}$ lineages under the $T_c = 0$ h and $T_c = 3$ h conditions and those observed under continuous exposure exclude $_{121}$ the possibility that growth restoration requires prior exposure to Cp before resistance gene deletion. $_{122}$

We next conjectured that a low amount of mCherry-CAT proteins is required at the onset of Cp exposure $_{123}$ to withstand and restore growth without the resistance gene. In fact, *mcherry-cat* gene deletion before Cp $_{124}$ exposure led to the dilution of mCherry-CAT proteins by growth by the time of Cp exposure (Fig. 3D and E). $_{125}$

To examine whether the mCherry-CAT concentration in individual cells affects growth restoration, we $_{126}$ divided the resistance-gene-deleted cell lineages into two groups under each condition (top 50% and bottom $_{127}$ 50%) based on their mCherry-CAT fluorescence intensities at the onset of Cp exposure. While we found no $_{128}$ significant differences in the $T_c = 0$ and 3 h conditions, the top 50% group produced 2.4-fold more $_{129}$ growth-restored cells than the bottom 50% group in the $T_c = 6$ h condition (Fig. 3F). In the $T_c = 10$ h $_{130}$ condition, we could barely detect the fluorescence signals from any cells (Fig. 3D and E), and no cells showed $_{131}$ growth restoration as mentioned above (Fig. 3F). These results suggest that a low level of residual $_{132}$ mCherry-CAT proteins is required at the onset of Cp exposure, but high amounts do not necessarily ensure $_{133}$ the growth restoration in all resistance-gene-deleted cells. Moreover, 40% could be considered as the $_{134}$ maximum frequencies at which cells can restore growth without the resistance gene. $_{135}$

Growth restoration accompanies the recovery of stoichiometric balance of ribosomal subunits

$_{136}$
$_{137}$

The results above demonstrated that the residual mCherry-CAT proteins are important for initiating the $_{138}$ transition to growth restoration without the resistance gene. However, the residual proteins cannot directly $_{139}$ support the growth in later generations under Cp exposure as their levels are eventually diluted with growth. $_{140}$ Indeed, the amounts of mCherry-CAT proteins during growth restoration were below the detection limit $_{141}$ (Fig. 2F and H). Therefore, we speculated that the other physiological changes were responsible for growth $_{142}$ restoration. $_{143}$

Because Cp targets the 50S ribosomal subunit [17], it is plausible that ribosomal states were modulated in $_{144}$ the duration beginning from resistance gene deletion to growth restoration. Hence, we constructed an *E. coli* $_{145}$ strain YK0136 that expressed fluorescently-tagged dual ribosomal reporters, RplS-mCherry and $_{146}$ RpsB-mVenus (Fig. 4A) [18]. RplS and RpsB are ribosomal proteins in the 50S and 30S subunits, $_{147}$ respectively. Their fluorescent reporters were utilized to probe the ribosomal subunit balance in living $_{148}$ cells [18]. YK0136 also harbors the *cat* resistance gene (not tagged with *mcherry*) between the upstream and $_{149}$ downstream *loxP* sequences on the chromosome, and the PA-Cre recombination system was expressed via the $_{150}$ plasmid (Fig. 4A). We confirmed that YK0136 showed MIC values almost equivalent to those of the YK0083 $_{151}$ strain (Fig. S3 and S8). Furthermore, 30-min blue-light illuminations provoked *cat*-gene deletion in 28.6% $_{152}$ (452/1587) of YK0136 cells, which was comparable to the frequency of *mcherry-cat*-gene deletion in YK0083 $_{153}$ (Fig. 3B). $_{154}$

We conducted time-lapse measurements of YK0136 cells in the mother machine and induced the deletion $_{155}$ of the resistance gene via blue-light illumination under continuous exposure to 15 μg/ml of Cp (Movie S4). $_{156}$ Since previous experiments showed that the resistance gene deletion decelerates cellular growth significantly, $_{157}$ the deletion of the *cat* gene in each cell lineage was evaluated based on the distinctive declines of cellular $_{158}$ elongation rates after the blue-light illumination. We validated this criterion by hierarchical time-series $_{159}$ clustering applied to the growth of YK0083 cells and mCherry-CAT fluorescence transitions (Fig. S9 and $_{160}$ Methods). $_{161}$
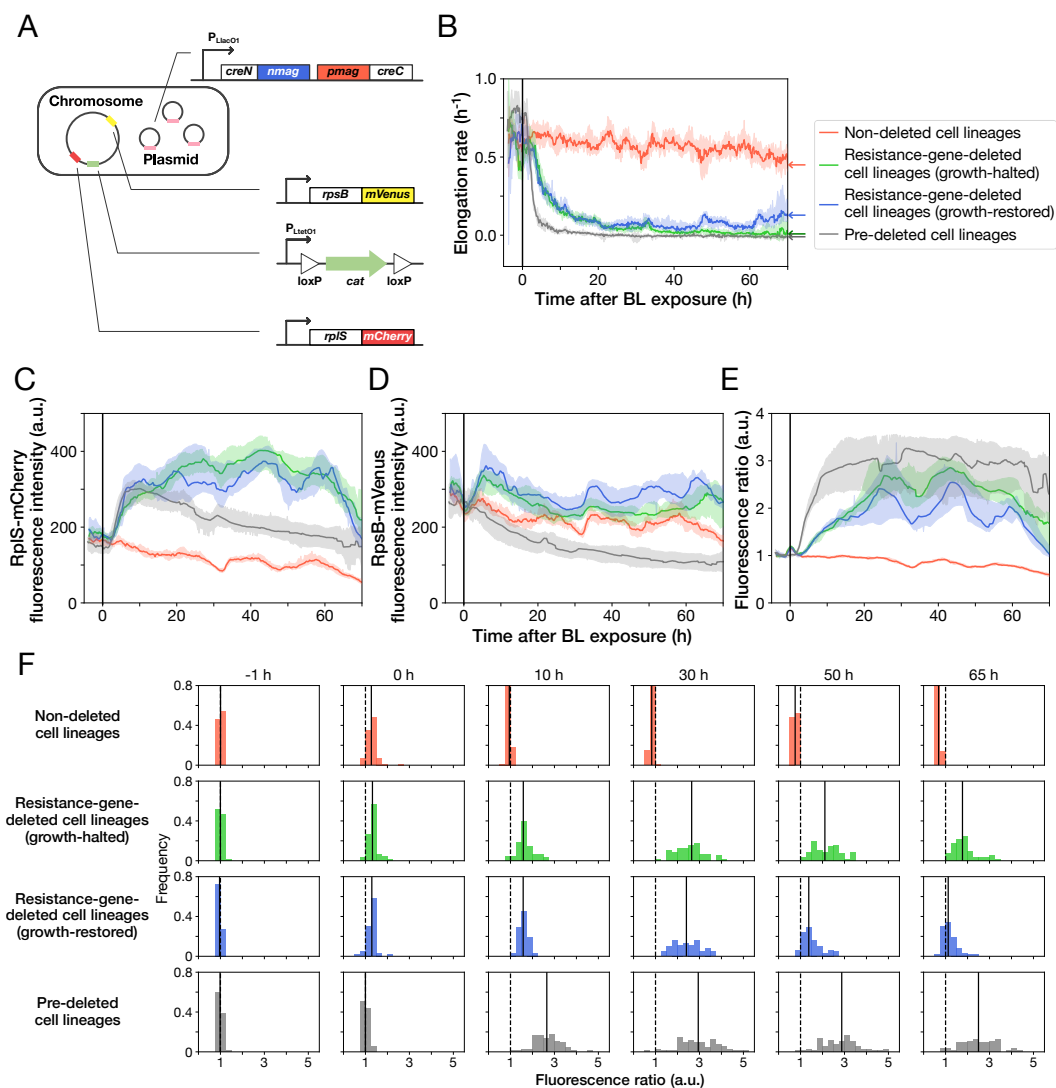
Figure 4. Disruption and restoration of ribosomal proteins' stoichiometry. (A) Schematic diagram of the ribosome reporter strain, YK0136. Fluorescently-tagged ribosomal protein genes ($rplS$ and $rpsB$) are expressed from the native loci on the chromosomes. Additionally, the photo-removable cat gene was integrated into the $intC$ locus on the chromosome. The PA-Cre fragments were expressed via low-copy plasmids. (B) Transitions of elongation rates. Lines represent the medians of elongation rates at each time point, and shaded areas show the 95% error ranges of the medians estimated by resampling the cell lineages 1,000 times. Red represents non-deleted cell lineages. Green shows growth-halted resistance-gene-deleted cell lineages. Blue represents growth-restored resistance-gene-deleted cell lineages. Gray represents pre-deleted cell lineages. Color correspondence remains the same in the following figures. The end of blue-light illumination was set to 0 h on the horizontal axis. (C-E) Transitions of RplS-mCherry fluorescence intensities (C), RpsB-mVenus fluorescence intensities (D), and the fluorescence ratio of RplS-mCherry/RpsB-mVenus (E). The fluorescence intensities of RplS-mCherry and RpsB-mVenus were normalized by the intensity observed at $t = 0$ h to calculate the ratio in E. (F) Transitions of the RplS-mCherry/RpsB-mVenus fluorescence ratio distributions. The vertical dashed lines represent the position of (ratio) = 1; the solid lines represent the medians of the distributions.
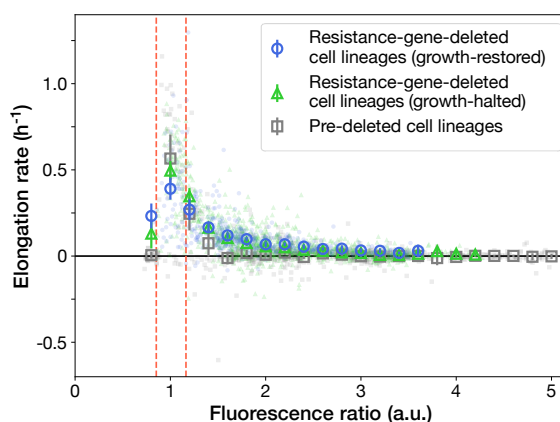
Figure 5. Scatter plot of fluorescence ratio and elongation rate under Cp exposure. Small points represent the relations between the fluorescence ratio and elongation rates averaged over the two-hour periods at the different time points on the single-cell lineages. The larger open point represents the mean elongation rate in each bin of fluorescence ratio (bin width, 0.2 a.u.). Error bars represent the $1.96\times$ standard error ranges. Blue represents growth-restored resistance-gene-deleted cell lineages. Green represents growth-halted resistance-gene-deleted cell lineages. Gray represents pre-deleted cell lineages. Red dashed lines indicate the mean $\pm$ $1.96\times$ standard error range of fluorescence ratio of non-deleted cell lineages before blue-light illumination.

As observed previously, 45.9% (158/344) of the *cat*-deleted YK0136 cells gradually restored their growth after initial growth suppression (Fig. 4B, S10 and Movie S4). Furthermore, such growth-restored cell lineages were not observed (0/1138) when YK0138 cells were exposed to 15 μg/ml of Cp; the YK0138 strain was constructed from YK0136 cells by deleting the *cat* gene beforehand in batch culture via blue-light illumination (Fig. 4B and Movie S5).

The transitions of fluorescence intensities reveal that *cat*-gene deletion under Cp exposure increased the expression levels of both RplS-mCherry and RpsB-mVenus (Fig. 4C and D). The relative changes triggered by deletion were more significant for RplS-mCherry than those for RpsB-mVenus (Fig. 4C and D). Consequently, the ribosomal subunit balance probed by the RplS-mCherry/RpsB-mVenus ratio was disrupted, and the ratio increased approximately 3-fold (Fig. 4E and F). The initial disruption kinetics was similar between growth-restored and growth-halted resistance-gene-deleted cell lineages (Fig. 4E). However, the ratio of growth-restored cell lineages gradually returned to the original level, whereas the ratio of growth-halted cell lineages remained disrupted (Fig. 4E and F). These results suggest that the regain of the ribosomal subunit balance under Cp exposure is required for growth restoration.

Analysis of the correlations between the pre-illumination phenotypic traits and post-illumination cellular fates reveals that elongation rates, fluorescence intensities of RplS-mCherry and RpsB-mVenus, and the fluorescence ratio observed before blue-light illumination did not strongly affect the likelihood of gene deletion and the determination of growth-halting and growth-restoration fates (Fig. S11).

When non-resistant YK0138 cells were exposed to 15 μg/ml of Cp, the expression levels of RplS-mCherry increased initially following kinetics similar to those of the YK0136 cells observed after *cat*-gene deletion (Fig. 4C). In contrast, the expression levels of RpsB-mVenus decreased in response to Cp exposure (Fig. 4D), as previously reported for a wildtype *E. coli* strain exposed to Cp [19]. The initial decrease of RpsB-mVenus expression led to a more rapid disruption of the RplS-mCherry/RpsB-mVenus ratio in the susceptible YK0138 cells (Fig. 4E and F). Consistently, the decline in the elongation rates of the YK0138 cells was faster than those of the YK0136 cells (Fig. 4B).

We further examined the relationship between the RplS-mCherry/RpsB-mVenus ratio and elongation rates and observed a negative correlation (Spearman ρ = -0.64, 95% confidence interval [-0.69,-0.58]; Fig. 5). The ratio was maintained within a narrow range (0.85-1.16, 95% interval) before blue-light illumination

(Fig. 4F and 5). The disruption of ribosomal subunit balance exceeding this range was linked to growth suppression (Fig. 5). These results suggest that the ribosomal subunit balance is essential for growth under Cp exposure and that cells must restore the balance to recover growth in the absence of the resistance gene.

Discussion

Uncovering the genotype-phenotype correspondences in various biological contexts is the groundwork for genetics. However, the correspondences are usually investigated based on terminal phenotypes, which are often manifested after significant lags following genotypic changes. Consequently, our understanding of the dependence of terminal phenotypes on historical conditions and the heterogeneity of phenotypic consequences among individual cells remains limited. In this study, we demonstrated that *E. coli* cells could adapt even to a lethal genetic modification, i.e., the deletion of *cat* resistance gene under exposure to chloramphenicol (Fig. 2). Importantly, such adaptation was not observed when an identical genetic modification was introduced long before Cp exposure (Fig. 3). Therefore, whether cells could gain physiological resistance in the absence of a resistance gene depends on the timing of resistance gene deletion and environmental histories that the cells experienced.

The analyses revealed that the *cat* gene deletion under Cp exposure disrupted the stoichiometric balance of ribosomal proteins (RplS and RspB) and that the balance was gradually recovered alongside growth restoration (Fig. 4). The elongation rate and the stoichiometric balance of ribosomal proteins were strongly correlated (Fig. 5). Furthermore, the balance was tightly regulated within a narrow range in the fast-growing non-deleted cells (Fig. 4F). Therefore, the recovery of ribosomal stoichiometric balance might be essential for restoring growth against the deletion of the resistance gene.

It still remains elusive how individual cells recovered the ribosomal stoichiometric balance under continuous Cp exposure. A plausible scenario might be that the multi-layered and interlinked feedback regulations on ribosomal components entailed stoichiometry readjustments [20–24]. Many ribosomal proteins bind to their own mRNAs, in addition to the target ribosomal RNAs [21–24]. These regulatory fractions of ribosomal proteins bind to their mRNAs and inhibit their own translation and that of other genes in the same operons. The competition among rRNA and mRNA for these regulatory ribosomal protein components is considered to regulate the stoichiometry of ribosomal components [21–24]. Therefore, it is plausible that these innate homeostatic mechanisms of ribosomes might have been exploited by cells to restore growth. It is also important to note that the operons for ribosomal proteins comprise genes encoding DNA polymerase subunits, initiation factors, and protein transmembrane transporters [22,23]. Hence, the feedback regulations in ribosomes could mediate changes in the global expression profiles, which might have helped the cells find growth-permissive states in the presence of Cp.

The necessity for a small amount of residual resistant proteins at the onset of Cp exposure (Fig. 3) might suggest that experiencing such barely-tolerable intracellular states is crucial for gaining physiological resistance. The importance of near-critical states for survival might be related to the phenomenon that pre-treatment with a sublethal concentration of antibiotics increases the fraction of persister cells in response to the subsequent treatments with lethal antibiotic concentrations [25,26]. Whether analogous mechanisms are involved in adaptation to both internal and external lethal perturbations is worth examining.

Though experimental evidence of history-dependent physiological adaptation to lethal genetic perturbations is still limited, the experimental strategy combining optogenetic recombination and single-cell lineage tracking is applicable for the modification of other genes or other cell types, including mammalian cells. Such approaches might offer new insights into the emergence of drug-resistant bacterial and cancer cells. Gaining a more comprehensive picture of resistance evolution might help us design new drug treatment strategies to counter or control the emergence and spread of resistance.

Acknowledgments

Materials and Methods 242

Bacterial strains, plasmids construction, and culture conditions   *E. coli* strains, plasmids, and ²⁴³
primers are listed in Table S2, S3, and S4, respectively. For strain constructions, cells were grown in Luria ²⁴⁴
Bertani (LB) broth (Difco) at 37°C unless stated otherwise. Plasmids were constructed using DNA ligase ²⁴⁵
(T4 DNA Ligase, Takara) or by ExoIII cloning [27] and introduced into the *E. coli* strain JM109 for cloning ²⁴⁶
and stocking. The *cat* or *mcherry-cat* gene was introduced into the *intC* locus of F3 ²⁴⁷
(W3110Δ*fliC*::FRTΔ*fimA*::FRTΔ*flu*::FRT) genome by λ-Red recombination (YK0080, YK0134) [28]. ²⁴⁸
Fluorescently-tagged ribosome reporter genes were introduced into the *E. coli* strain BW25113 (MUS3, ²⁴⁹
MUS13). These ribosome reporter genes were transferred into the F3 strain by P1 transduction (MUS5, ²⁵⁰
MUS6). The colonies with intended genome integration were selected on LB plates containing kanamycin ²⁵¹
(Km, Wako). The Km resistant gene was removed by flp-FRT recombination using pCP20 plasmid [28]. ²⁵²

When constructing the resistance-gene-deleted strains (YK0085 and YK0138), YK0083 and YK0136 cells ²⁵³
were pre-cultivated overnight in LB broth containing 50 μg/mL of ampicillin (Amp, Wako). 10 μL of ²⁵⁴
overnight cultures were inoculated into 2 mL of the M9 medium containing 50 μg/mL of Amp and 0.1 mM ²⁵⁵
isopropyl-β-D-thiogalactopyranoside (IPTG, Wako) in test tubes. The cell cultures were cultivated at 37°C ²⁵⁶
with shaking. After a 3 h cultivation period for inducing the expression of PA-Cre system by IPTG, the ²⁵⁷
batch cultures were illuminated by LED blue light (CCS) for 24 h. The light intensity was adjusted to 6.8 ²⁵⁸
mW, which is equivalent to the intensity in the microscopy experiments. The cell cultures were streaked on ²⁵⁹
LB agar containing 100 μg/mL of Amp. The plates were incubated at 37°C overnight. After overnight ²⁶⁰
incubation, several colonies were selected. The deletion of the intended gene in these colonies was examined ²⁶¹
via PCR. The colonies with the intended gene deletion were cultured in LB medium containing 50 μg/mL of ²⁶²
Amp at 37°C. These cell cultures were stored at -80°C as glycerol stocks. ²⁶³

The genomes of the constructed strains and plasmids were purified using the Promega Genomic DNA ²⁶⁴
Purification kit and the Promega Plasmid Miniprep System, respectively, and the DNA sequence of the ²⁶⁵
modified locus was amplified by Prime STAR (Takara). The sequence was examined by Sanger sequencing ²⁶⁶
using a commercial service (FASMAC). ²⁶⁷

In microscopy experiments, we used M9 minimal medium, which consisted of M9 salt (Difco), 2 mM ²⁶⁸
MgSO$_4$ (Wako), 0.1 mM CaCl$_2$ (Wako), 0.2% (w/v) glucose (Wako) and 0.2%(v/v) MEM amino acid (50x) ²⁶⁹
solution (Sigma). When necessary, antibiotics and chemicals were added at the following final concentrations ²⁷⁰
unless otherwise noted: Amp 50 μg/mL, Km 20 μg/mL, chloramphenicol (Cp, Wako) 15 μg/mL, and IPTG ²⁷¹
0.1 mM. ²⁷²

Calculation of the fraction of resistance-gene-deleted cells in batch culture   YK0083 cells were ²⁷³
pre-cultivated in LB broth containing 50 μg/mL of Amp overnight. 100 μL of the overnight culture was spun ²⁷⁴
at 21,500 $\times g$ for 1 minute by a centrifuge (CT15E, himac, Hitachi) and resuspended in 1 mL of the M9 ²⁷⁵
minimal medium. This culture was inoculated in 2 mL of the M9 medium containing 50 μg/mL of Amp and ²⁷⁶
0.1 mM IPTG (except for the "no IPTG" condition) in test tubes covered with aluminum foil for light ²⁷⁷
protection. The starting OD$_{600}$ was adjusted to 0.001, and the cells were cultivated at 37°C with shaking. ²⁷⁸
After a 3 h cultivation period for inducing the expression of the PA-Cre system by IPTG, the aluminum foil ²⁷⁹
cover was removed, and the test tubes were exposed to blue light. The light intensity was adjusted to 6.8 ²⁸⁰
mW. The illumination length was determined according to the experimental conditions (Fig. S2B). For the ²⁸¹
conditions with an illumination duration of less than 6 h, the test tubes were again covered with aluminum ²⁸²
foil and incubated with shaking so that the total cultivation duration from the start of blue-light illumination ²⁸³
was identical (6 h) across all conditions. Under the "no IPTG" condition, the test tubes were covered with ²⁸⁴
the aluminum foil throughout the incubation period and were not exposed to blue light. ²⁸⁵

For calculating the fractions of resistance-gene-deleted cells, the cultures exposed to blue-light were diluted to $OD_{600} = 1.0 \times 10^{-6}$, and 150 μL of the diluted cultures was spread on LB agar containing 100 μg/mL of Amp. The plates were incubated at 37°C for 18 h. After incubation, the number of colonies was counted under ambient light or excitation light for examining mCherry fluorescence using stereomicroscope (stereomicroscope: Olympus SZ61; LED source: NIGHTSEA SFA-GR). The fraction of resistance-gene-deleted cells was calculated as the number of non-fluorescent colonies divided by the number of total colonies (Fig. S2B). To validate this classification, we conducted colony PCR and checked whether the designed deletion was introduced (Fig. S2C).

Sample preparation and experimental procedures for MIC tests   Cells stored as a glycerol stock were inoculated in the LB broth (Fig. S3, and S8) or the M9 medium (Fig. S6C) containing 50 μg/mL of Amp. The cells were cultured at 37°C with shaking overnight. 100 μL of overnight culture was centrifuged at 21,500$\times g$ for 3 min. The supernatant was discarded, and the cells were resuspended in 1.0 mL of the M9 medium. This culture was diluted to the cell density corresponding to $OD_{600} = 0.01$ in the M9 medium containing 50 μg/mL of Amp and incubated with shaking for 3-4 h at 37°C. The cell culture was again diluted to $OD_{600} = 0.001$ in fresh M9 media containing different concentrations of Cp (Fig. S3, S6C and S8). After 23 h of incubation, the OD_{600} of these cultures was measured with a spectrometer (UV-1800, Shimadzu) in Fig. S3 and S8 or with a multi-mode microplate reader (FilterMax F5, Molecular Devices) in Fig. S6C.

Microfabrication of Mother Machine microfluidic device   We created two chromium photomasks, one for the main trench and the other for the observation channels, by laser drawing (DDB-201-TW, Neoark) on mask blanks (CBL4006Du-AZP, Clean Surface Technology). The photoresist on mask blanks was developed in NMD-3 (Tokyo Ohka Kogyo), and the uncovered parts of the chromium layer were removed by MPM-E30 (DNP Fine Chemicals). The remaining photoresist was removed by acetone. The photomasks were rinsed in MilliQ water and air-dried.

We created the mold for the mother machine on a silicon wafer (ID447, ϕ=76.2 mm, University Wafer). First, we spin-coated SU8-2 (MicroChem) on the wafer with the target height of 1.2 μm. The SU8-coated wafer was baked at 65°C for 1 min and thereafter at 95°C for 3 min. The SU8-layer was exposed to UV light thrice (each exposure, 22.4 mW/cm^2, 1.7 sec) using a mask aligner (MA-20, Mikasa). The photomask for the observation channels was used in this step. The wafer was post-baked at 65°C for 1 min and 95°C for 3 min after the exposure and developed with the SU8 developer. The wafer was rinsed with isopropanol (Wako) and air-dried.

Next, we spin-coated SU8-3025 (MicroChem) with the target height of 20 μm. The pre-bake was performed at 65°C for 3 min and thereafter at 95°C for 7 min. The SU-8 layer was again exposed to UV light (22.4 mW/cm^2, 30 sec) with the photomask for the main trench. The wafer was post-baked at 65°C for 3 min and 95°C for 10 min and developed with the SU8 developer. The wafer was rinsed with isopropanol and air-dried.

The Part A and Part B of polydimethylsiloxane (PDMS) resin (Sylgard 184 Silicone Elastomer Kit, Dow Corning) were mixed at the ratio of 10:1 and poured onto the SU-8 mold placed in a tray made of aluminum foil. After removing the air bubbles under decreased pressure, the PDMS was cured at 65°C for 1 h. We cut out a PDMS block containing the channel structures and punched holes at both ends of the main trench. The PDMS block was washed with isopropanol and heated at 65°C for 30 min.

We washed the coverslips (thickness: 0.13-0.17 mm, 24 $\times$ 60 mm, Matsunami) by sonication with 10-fold-diluted Contaminon solution (Contaminon® LS-Ⅱ, Wako) for 30 min, with 99.5% ethanol (Wako) for 15 min, and with 0.8 M NaOH solution (10-fold diluted 8 M NaOH (Wako)) for 30 min. The coverslips were rinsed with milliQ water by sonication after each washing step. The coverslips were dried at 140°C for 1 h. We exposed the PDMS block and the coverslips to oxygen plasma using a compact etcher (FA-1, SAMCO) and bonded them together at 65°C for 5 min. After bonding, we inserted the silicone tubes (inner diameter: 1 mm, outer diameter: 2 mm, Tigers Polymer Corporation) into the holes and smeared a small amount of pre-cured PDMS. We cured the PDMS at 65°C overnight to fix the tubes into the holes tightly.

Sample preparation and experimental procedures for single-cell time-lapse experiments Cells stored as a glycerol stock were inoculated in the LB broth containing 50 μg/mL of Amp and cultured at 37°C overnight with shaking (200 rpm). 200 μL of overnight culture was centrifuged at 21,500$\times g$ for 3 min. The supernatant was discarded, and the cells were resuspended in 1.5 mL of the M9 medium. This culture was diluted to $OD_{600} = 0.01$ in the M9 medium containing 50 μg/mL of Amp, and incubated with shaking for 5-6 h at 37°C. The cell culture was again spun at 2,350$\times g$ for 5 min using a centrifuge (CT6E, himac, Hitachi), and the cells were resuspended in 200 μL of the M9 medium.

Before loading the cells, the growth channels and the main trench in the mother machine device were washed by flowing 0.5 mL of 99.5% ethanol, M9 medium, and 1% (w/v) bovine serum albumin (BSA, Wako) solution sequentially using a syringe. After washing, we introduced the cell suspension into the device and let the cells enter the growth channels by placing the device at 37°C for 1-2 h without flow in a dark room. After confirming that the cells were trapped in many growth channels, we started flowing the M9 medium containing 0.1 mM IPTG and 0.1% (w/v) BSA at 2 mL/h. For experiments with continuous Cp exposure, we also added 15 μg/mL of Cp to the flowing medium from the beginning. We initiated time-lapse image acquisitions after overnight cultivation in the mother machine. We illuminated blue light for 30 min at pre-determined timings in all single-cell time-lapse experiments. The medium flow rate was maintained at 2 mL/h and increased to 5 mL/h for 30 min once or twice a day to prevent the formation of cell aggregates in the main trench.

Time-lapse image acquisitions and analysis Time-lapse image acquisitions were performed with ECLIPSE Ti fluorescent microscope (Nikon) equipped with 100$\times$ oil immersion objective lens (Plan Apo λ, NA 1.45, Nikon), digital CMOS camera (ORCA-frash, Hamamatsu Photonics), and LED light source (DC2100, Thorlabs) for fluorescence excitation. For acquiring phase-contrast images, the transmitted light was illuminated for 20 msec during *mcherry-cat* gene deletion experiments and for 50 msec during experiments performed with ribosome reporter strains through neutral density and red filters to avoid unintended activation of PA-Cre. Fluorescence images were acquired with appropriate filter cubes (YFP HQ (Nikon) for mVenus and Texas Red (Nikon) for mCherry). In the *mcherry-cat* gene deletion experiments, mCherry fluorescence was obtained every 2 min with excitation of 500 msec. The mCherry and mVenus fluorescence images were acquired every 10 min with the excitation of 100 msec in the experiments with ribosome reporter strains. IPTG was removed from the flowing media after blue-light illumination to avoid unintended gene deletion.

Blue-light illumination on the microscope for gene deletion experiments was regulated by an independent controller. We used a tape LED (7.2 mW, wave length:464~474 nm, 60 LED/1 m, LED PARADISE) as the blue-light source and surrounded the mother machine device on the microscope stage with this tape LED. The LED light was switched on and off with a timer (REVEX).

Image analysis was performed using ImageJ Fiji (http://fiji.sc/). Image registration was performed by HyperStackReg described in MoMA Macro [29]. Cell segmentation was semi-automated and retouched manually using iPad Pro Sidecar. Semi-automated segmentation and tracking Macro reported previously [30] were used in this study. The data from image analysis were further analyzed using Python 3 (https://www.python.org/) with some general packages, including NumPy, SciPy, pandas, Matplotlib, seaborn, FastDTW, and JupyterLab.

The transitions of mCherry-CAT fluorescence intensities and elongation rates in single-cell lineages were classified using hierarchical clustering in Fig. S9. The full-length single-cell lineage data were used in this analysis. The similarity of each pair of time series was measured by dynamic time warping [31]. Hierarchical clustering is agglomerative; the averaged dynamic time warping was used when similarity to another time series or cluster was evaluated.

Cell sampling from the mother machine and whole-genome sequencing After time-lapse observations performed with the mother machine, we switched the flowing media to the M9 medium containing 0.1% (w/v) BSA and no Cp. We recovered the growth of growth-restored resistance-gene-deleted cell lineages by culturing them without Cp for more than 6 h. Subsequently, we collected the media flowing out from the mother machine in a 1.5-mL tube. The OD_{600} of the collected cell suspension was measured

with a spectrometer (UV-1800, Shimadzu). The cell suspension was diluted serially with the M9 medium to obtain a cell density corresponding to $OD_{600} = 3.3 \times 10^{-9}$. 200 μL of diluted cell suspension was taken in each well of 96-well plates. The number of cells in the 200 μL of cell suspension k is expected to follow a Poisson distribution $P(k) = \lambda^k e^{-\lambda}/k!$ with the mean $\lambda = 0.54$. Therefore, $P(0) = 0.58$, $P(1) = 0.31$, $P(2) = 0.085$, and $P(k \geq 3) = 0.018$. The 96-well plates were incubated with shaking at 37°C for two nights. We performed PCR on samples with high turbidity in wells to confirm the presence or absence of the *cat* gene. We selected both *cat*-positive and *cat*-negative cellular populations from the 96-well plates and cultured them in test tubes overnight at 37°C. We stored these samples at -80°C for further analyses.

For the measurement of mCherry-CAT fluorescence intensities of the selected samples (Fig. S6), cells stored as a glycerol stock were inoculated in the M9 medium containing 50 μg/mL of Amp and cultured at 37°C with shaking (200 rpm) overnight. 10 μL of overnight culture was inoculated in the M9 medium containing 50 μg/mL of Amp and incubated with shaking for 4 h at 37°C. 0.3 μL of cell culture was placed on an agar pad prepared using the M9 medium and 1.5% (w/v) agar (Wako) and covered with a coverslip. Image acquisitions of the samples were performed with ECLIPSE Ti fluorescent microscope (Nikon) equipped with 100× oil immersion objective lens (Plan Apo λ, NA 1.45, Nikon), digital CCD camera (ORCA-R2, Hamamatsu Photonics), and LED light source (DC2100, Thorlabs) for fluorescence excitation. For acquiring phase-contrast images, the transmitted light was illuminated for 50 msec through neutral density. The mCherry fluorescence images were acquired with Texas Red filter cubes and an exposure time of 500 msec.

For the measurement of whole-genome sequencing of the selected samples, cells stored as a glycerol stock were inoculated in 5 mL of the M9 medium and cultured at 37°C with shaking (200 rpm) overnight. The OD_{600} of overnight culture was measured with a spectrometer. Rifanpicin (Wako) was added to the overnight culture to the final concentration of 300 μg/mL. After 3 h of incubation, the genomes of these samples were extracted with DNeasy Blood and Tissue kit (QIAGEN). TruSeq DNA PCR Free kit (Illumina) was used for the whole-genome sequencing library preparation. These libraries were sequenced using NovaSeq (Illumina). Library preparation and sequencing were outsourced to Macrogen Japan (Tokyo, Japan). The sequence data were analyzed with breseq [32].

References

1. Battesti A, Majdalani N, Gottesman S. The RpoS-mediated general stress response in Escherichia coli. Ann Rev Microbiol. 2011;34:189–213. doi:10.1146/annurev-micro-090110-102946.

2. Walker GC. The SOS Response of Escherichia coli. In: Neidhardt FC, editor. Escherichia coli and Salmonella: Cellular and Molecular Biology. 2nd ed. ASM Press; 1996.

3. Taddei F, Matic I, Radman M. cAMP-dependent SOS induction and mutagenesis in resting bacterial populations. Proceedings of the National Academy of Sciences of the United States of America. 1995;92:11736–40. doi:10.1073/pnas.92.25.11736.

4. Ryan FJ. Phenotypic (Phenomic) Lag in Bacteria. The American Naturalist. 1955;89:159–162. doi:10.1086/281875.

5. Sun L, Alexander HK, Bogos B, Kiviet DJ, Ackermann M, Bonhoeffer S. Effective polyploidy causes phenotypic delay and influences bacterial evolvability. PLoS Biology. 2018;16(2):e2004644. doi:10.1371/journal.pbio.2004644.

6. Waddington CH. Canalization of development and the inheritance of acquired characters. Nature. 1942;150(3811):563–565. doi:10.1038/150563a0.

7. Rutherford SL, Lindquist S. Hsp90 as a capacitor for morphological evolution. Nature. 1998;396(6709):336–342. doi:10.1038/24550.

8. Queitsch C, Sangstert TA, Lindquist S. Hsp90 as a capacitor of phenotypic variation. Nature. 2002;417(6889):618–624. doi:10.1038/nature749.

9. Fares MA, Ruiz-González MX, Moya A, Elena SF, Barrio E. Endosymbiotic bacteria: GroEL buffers against deleterious mutations. Nature. 2002;417(6887):398. doi:10.1038/417398a.   429 430

10. El-Brolosy MA, Stainier DYR. Genetic compensation: A phenomenon in search of mechanisms. PLoS Genetics. 2017;13(7):e1006780. doi:10.1371/journal.pgen.1006780.   431 432

11. Eldar A, Chary VK, Xenopoulos P, Fontes ME, Losón OC, Dworkin J, et al. Partial penetrance facilitates developmental evolution in bacteria. Nature. 2009;460:510–4. doi:10.1038/nature08150.   433 434

12. Kawano F, Okazaki R, Yazawa M, Sato M. A photoactivatable Cre-loxP recombination system for optogenetic genome engineering. Nature Chemical Biology. 2016;12(12):1059–1064. doi:10.1038/nchembio.2205.   435 436 437

13. Wang P, Robert L, Pelletier J, Dang WL, Taddei F, Wright A, et al. Robust growth of escherichia coli. Current Biology. 2010;20(12):1099–1103. doi:10.1016/j.cub.2010.04.045.   438 439

14. Shaw WV. The enzymatic acetylation of chloramphenicol by extracts of R factor-resistant Escherichia coli. The Journal of Biological Chemistry. 1967;242(4):687–93.   440 441

15. Kawano F, Suzuki H, Furuya A, Sato M. Engineered pairs of distinct photoswitches for optogenetic control of cellular proteins. Nature Communications. 2015;6(7):6256. doi:10.1038/ncomms7256.   442 443

16. Milo R. What is the total number of protein molecules per cell volume? A call to rethink some published values. BioEssays. 2013;35:1050–1055. doi:10.1002/bies.201300066.   444 445

17. Pongs O. Chloramphenicol. In: Mechanism of Action of Antibacterial Agents. Berlin, Heidelberg: Springer Berlin Heidelberg; 1979. p. 26–42. Available from: http://link.springer.com/10.1007/978-3-642-46403-4{_}3.   446 447 448

18. Nikolay R, Schloemer R, Schmidt S, Mueller S, Heubach A, Deuerling E. Validation of a fluorescence-based screening concept to identify ribosome assembly defects in Escherichia coli. Nucleic Acids Research. 2014;42(12):e100. doi:10.1093/nar/gku381.   449 450 451

19. Siibak T, Peil L, Dönhöfer A, Tats A, Remm M, Wilson DN, et al. Antibiotic-induced ribosomal assembly defects result from changes in the synthesis of ribosomal proteins. Molecular Microbiology. 2011;80(1):54–67. doi:10.1111/j.1365-2958.2011.07555.x.   452 453 454

20. Yamagishi M, Nomura M. Effects of induction of rRNA overproduction on ribosomal protein synthesis and ribosome subunit assembly in Escherichia coli. Journal of bacteriology. 1988;170(11):5042–5050. doi:10.1128/jb.170.11.5042-5050.1988.   455 456 457

21. Nomura M, Gourse R, Baughman G. Regulation of the synthesis of ribosomes and ribosomal components. Annual Review of Biochemistry. 1983;53:75–117. doi:10.1146/ANNUREV.BI.53.070184.000451.   458 459 460

22. Lindahl L, Zengel JM. Ribosomal genes in Escherichia coli. Annual Reviews of Genetics. 1986;20:297–326. doi:10.1146/ANNUREV.GE.20.120186.001501.   461 462

23. Keener J, Nomura M. Regulation of Ribosome Synthesis. In: Neidhardt FC, editor. Escherichia coli and Salmonella: Cellular and Molecular Biology. ASM Press; 1996.   463 464

24. Kaczanowska M, Rydén-Aulin M. Ribosome Biogenesis and the Translation Process in Escherichia coli. Microbiology and Molecular Biology Reviews. 2007;71:477–494. doi:10.1128/MMBR.00013-07.   465 466

25. Dörr T, Lewis K, Vulić M. SOS response induces persistence to fluoroquinolones in Escherichia coli. PLoS Genetics. 2009;5(12):e1000760. doi:10.1371/journal.pgen.1000760.   467 468

26. Johnson PJT, Levin BR. Pharmacodynamics, Population Dynamics, and the Evolution of Persistence in Staphylococcus aureus. PLoS Genetics. 2013;9(1):e1003123. doi:10.1371/journal.pgen.1003123.   469 470

27. Li C, Evans RM. Ligation independent cloning irrespective of restriction site compatibility. Nucleic Acids Research. 1997;25(20):4165–4166. doi:10.1093/nar/25.20.4165.

28. Datsenko KA, Wanner BL. One-step inactivation of chromosomal genes in Escherichia coli K-12 using PCR products. Proceedings of the National Academy of Sciences of the United States of America. 2000;97(12):6640–6645. doi:10.1073/pnas.120163297.

29. Kaiser M, Jug F, Julou T, Deshpande S, Pfohl T, Silander OK, et al. Monitoring single-cell gene regulation under dynamically controllable conditions with integrated microfluidics and software. Nature Communications. 2018;9(1):212. doi:10.1038/s41467-017-02505-0.

30. Hashimoto M, Nozoe T, Nakaoka H, Okura R, Akiyoshi S, Kaneko K, et al. Noise-driven growth rate gain in clonal cellular populations. Proceedings of the National Academy of Sciences of the United States of America. 2016;113(12):3151–3156. doi:10.1073/pnas.1519412113.

31. Salvador S, Chan P. Toward accurate dynamic time warping in linear time and space. Intelligent Data Analysis. 2007;11(5):561–580. doi:10.3233/ida-2007-11508.

32. Deatherage DE, Barrick JE. Identification of mutations in laboratory-evolved microbes from next-generation sequencing data using breseq. Methods in Molecular Biology. 2014;1151:165–188. doi:10.1007/978-1-4939-0554-6_12.

Supplemental Information 487

Supplemental Movies 488

Movie S1. Deletion of *mcherry-cat* gene by blue-light illumination under drug-free 489
conditions.   YK0083 cells were cultured in the mother machine flowing the M9 minimal medium and 490
exposed to blue light from $t = $ -30 min to 0 min (marked with "+ BL"). The merged images of phase 491
contrast (grayscale) and mCherry-CAT fluorescence (red) channels are shown. The fluorescence of 492
mCherry-CAT was gradually lost after blue-light illumination in this cell lineage. Scale bar, 5 μm. 493

Movie S2. Growth restoration under Cp exposure after resistance gene deletion.   YK0083 494
cells were cultured in the mother machine flowing the M9 minimal medium containing 15 μg/mL of Cp. Blue 495
light was illuminated from $t = $ -30 min to 0 min (marked with "+ BL"). The merged images of phase 496
contrast (grayscale) and mCherry-CAT fluorescence (red) channels are shown. The illumination caused the 497
loss of fluorescence signals, i.e., the deletion of the *mcherry-cat* gene, in this cell lineage. Nevertheless, the 498
cell gradually restored growth and division under continuous Cp exposure. Scale bar, 5 μm. 499

Movie S3. No growth recovery of YK0085 strain under Cp exposure.   YK0085 cells were 500
cultured in the mother machine flowing the M9 minimal medium and exposed to 15 μg/mL of Cp at $t = 0$ 501
min (marked with "+ Cp"). The Cp exposure caused growth arrest, and, unlike the YK0083 cells, the cell 502
did not restore growth. We found no growth-restored cell lineages in this experimental condition. Scale bar, 503
5 μm. 504

Movie S4. Recovery of the balance of ribosomal proteins alongside growth restoration. 505
YK0136 cells were cultured in the mother machine flowing the M9 minimal medium containing 15 μg/mL of 506
Cp. Blue light was illuminated from $t = $ -30 min to 0 min (marked with "+ BL"). The merged images of 507
phase contrast (grayscale), RplS-mCherry fluorescence (red), and RpsB-mVenus fluorescence (green) 508
channels are shown. The growth of the cell markedly slowed down after blue-light illumination, indicating 509
the loss of the *cat* gene. The cell became red in response to blue-light illumination, indicating that the 510
relative expression level of RplS-mCherry became higher than that of RpsB-mVenus. However, the balance 511
was restored alongside growth restoration. Scale bar, 5 μm. 512

Movie S5. No recovery of the balance of ribosomal proteins in the YK0138 strain.   YK0138 513
cells were cultured in the mother machine flowing the M9 minimal medium and exposed to 15 μg/mL of Cp 514
at $t = 0$ min (marked with "+ Cp"). The Cp exposure caused growth arrest and disruption of ribosomal 515
proteins' expression balance. No restoration of growth and ribosomal balance was observed. Scale bar, 5 μm. 516

Supplemental Tables

Table S1. Mutations detected by whole-genome sequencing. We obtained isolated cellular populations derived from single or few cells by limiting dilution of the culture media flowing out from the mother machine. We detected only one point mutation in Sample 3.

Sample No.	Mutation	Position	Base	Annotation
Sample 1	no mutation			
Sample 2	no mutation			
Sample 3	mutation in leuC site	80471	G ->T	A132S
Sample 4	no mutation			
Sample 5	no mutation			

Table S2. Strain list used in this study.

mCherry-CAT deletion

Name	Genotype	Sourse
F3	W3110 $\Delta fliC$::FRT$\Delta fimA$::FRTΔflu::FRT	[30]
YK0080	F3 $intC$::P_{LtetO1}-loxp-RBS4-$mcherry$-cat-loxp-FRT	This study
YK0083	F3 $intC$::P_{LtetO1}-loxp-RBS4-$mcherry$-cat-loxp-FRT/pYK022	This study
YK0085	F3 $intC$::P_{LtetO1}-FRT/pYK022	This study

Ribosome reporter

Name	Genotype	Sourse
MUS3	BW25113 $rplS$-$mcherry$-FRT-kan-FRT	This study
MUS13	BW25113 $rpsB$-$mvenus$-FRT-kan-FRT	This study
MUS5	F3 $rplS$-$mcherry$-FRT	This study
MUS6	F3 $rplS$-$mcherry$-FRT $rpsB$-$mvenus$-FRT	This study
YK0134	MUS6 $intC$::P_{LtetO1}-loxP-RBS4-cat-loxP-FRT	This study
YK0136	MUS6 $intC$::P_{LtetO1}-loxP-RBS4-cat-loxP-FRT/pYK022	This study
YK0138	MUS6 $intC$::P_{LtetO1}-loxP-FRT/pYK022	This study

Table S3. Plasmid list used in this study.

Name	Backbone	Gene	Sourse
pKD46			CGSC
pCP20			CGSC
	pcDNA3.1	pCMV-lox2272-loxp-inversed *mvenus*-lox2272-loxp	Sato lab
	pcDNA3.1	pCMV-rfp-*pmag-creC*	Sato lab
	pcDNA3.1	pCMV-rfp-*nmag-creN*	Sato lab
pTmCherryK3	pMW118	P_{LtetO1}-RBS3-*mcherry*-FLP-*kan*-FLP	Wakamoto lab
pLVK4	pMW118	P_{LlacO1}-RBS4-*mvenus*-FLP-*kan*-FLP	Wakamoto lab
pTVCK4	pMW118	P_{LtetO1}-RBS4-*mvenus-cat*-FLP-*kan*-FLP	Wakamoto lab
pKK1	pMW118	P_{LlacO1}-rfp-*pmag-creC*-FLP-*kan*-FLP	This study
pKK2	pMW118	P_{LlacO1}-rfp-*nmag-creN*-FLP-*kan*-FLP	This study
pYK001	pMW118	P_{LlacO1}-RBS3-*pmag-creC*-FLP-*kan*-FLP	This study
pYK002	pMW118	P_{LlacO1}-RBS3-*nmag-creN*-FLP-*kan*-FLP	This study
pYK006	pMW118	P_{LtetO1}-RBS3-lox2272-*mvenus*-loxp-FLP-*kan*-FLP	This study
pYK007	pMW118	P_{LtetO1}-RBS3-lox2272-*mcherry*-loxp-FLP-*kan*-FLP	This study
pYK008	pMW118	P_{LtetO1}-RBS3-lox2272-*mcherry*-loxp-FLP-*kan*-FLP	This study
pYK009	pMW118	P_{LtetO1}-RBS3-lox2272-*mcherry*-loxp-FLP-*kan*-FLP	This study
pYK010	pMW118	P_{LtetO1}-RBS4-lox2272-*mcherry*-loxp-FLP-*kan*-FLP	This study
pYK011	pMW118	P_{LtetO1}-lox2272-RBS4-*mcherry*-loxp-FLP-*kan*-FLP	This study
pYK016	pMW118	P_{LlacO1}-RBS3-*pmag-creC*-FLP-*kan*-FLP	This study
pYK017	pMW118	P_{LlacO1}-RBS3-*creN-nmag*-FLP-*kan*-FLP	This study
pYK018	pMW118	P_{LlacO1}-RBS3-*creN-nmag-pmag-creC*-FLP-*kan*-FLP	This study
pYK022	pMW118	P_{LlacO1}-RBS3-*creN-nmag-pmag-creC*-FLP-*kan*-FLP	This study
pYK023	pMW118	P_{LtetO1}-loxp-RBS4-*mcherry*-loxp-FLP-*kan*-FLP	This study
pYK028	pMW118	P_{LtetO1}-loxp-RBS4-*mcherry*-loxp-FLP-*kan*-FLP	This study
pYK029	pMW118	P_{LtetO1}-loxp-RBS4-*mcherry-cat*-loxp-FLP-*kan*-FLP	This study
pYK035	pMW118	P_{LtetO1}-loxp-RBS4-*cat*-loxp-FLP-*kan*-FLP	This study
pMU1	pMW118	P_{LlacO1}-RBS4-*mcherry*-FLP-*kan*-FLP	This study
pMU2	pMW118	P_{LlacO1}-RBS4-*mvenus*-FLP-*kan*-FLP	This study

Table S4. Primer list used in this study.

PA-Cre plasmid construction

Name	Sequence	Usage
pLVK_pTVK_F	CAGGCATCAAATAAAACGAAAGGCTCAGTC	For constructing pKK1 and pKK2 plasmids using ExoIII cloning [27]. Templates: pLVK3 (pLVK_pTVK_F & pLVK3_pTVK3_R), pCMV-rfp-pmag-creC (L3_TagRFP_F & Crec_Term_R), and pCMV-rfp-nmag-creN (L3_TagRFP_F & 141031-nMagCreN-R)
pLVK3_pTVK3_R	GGTACCTTTCTCCTCTTTAATGTTTTCGG	
L3_TagRFP_F	GGACGCACTGACCGAAAACATTAAAGAGGAGAAAGGTACCATGGTGTCTAAGGGCGAAG	
Crec_Term_R	CCAGTCTTTCGACTGAGCCTTTCGTTTTATTTGATGCCTGTTAGTCCCCATCTTCGAGCAG	
141031-nMagCreN-R	TTCGTTTTATTTGATGCCTGTTAGTTCAGCTTGCACCAGG	
YKp0001	ATGCATACTCTTTATGCCCCCGG	For constructing pYK001 and pYK002 plasmids by removing the *rfp* gene from pKK1 and pKK2.
YKp0002	GGTACCTTTCTCCTCTTTAATG	
YKp0053	AACAGGAAATGGTTCCCTGCTGAACC	For constucting pYK016 plasmid by changing the linker between *pmag* and *creC* on pYK001.
YKp0054	GGTACCTTCTGTTTCGCACTGGAATC	
YKp0022	GTGTAGGCTGGAGCTGCTTCG	For constructing pYK017 plasmid using ExoIII cloning. PCR was conducted with the template pYK002 using YKp0022 & YKp0052, YKp0049 & YKp0056 and YKp0055 & YKp0057 to change the order of *nmag* and *creN*.
YKp0049	AAGAGGAGAAAGGTACCATGACCTCTGATGAAGTCAGG	
YKp0052	CATGGTACCTTTCTCC	
YKp0055	CATACTCTTTATGCCCCCGGTGG	
YKp0056	GCATAAAGAGTATGGGTACCGTTCAGCTTGCACCAG	
YKp0057	CTCCAGCCTACACTTATTCTGTTTCGCACTGGAATC	
YKp0058	TTATTCTGTTTCGCACTGGAATCCC	For constructing pYK018 plasmid using ExoIII cloning. PCR was conducted on the template pYK016 with YKp0059 & YKp0060 and pYK017 with YKp0022 & YKp0058 to combine *pmag-creC* and *creN-nmag*.
YKp0059	GCGAAACAGAATAAAGGAGAAAGGTACCATGCATAC	
YKp0060	GCTCCAGCCTACACTTAGTCCCCATCTTCGAGCAGC	
YKp0006	CAGGCATCAAATAAAACGAAAGGCTCAGTCG	For constructing pYK022 plasmid using ExoIII cloning. PCR was conducted on the template pYK001 with YKp0006 & YKp0052 and pYK018 with YKp0049 & YKp0061 to add a terminator.
YKp0061	TTATTTGATGCCTGTTAGTCCCCATCTTCGAGCAGC	

Floxed *cat* plasmid construction

Name	Sequence	Usage
YKp0026	CGTTTTATTTGATGCCTGATAACTTCGTATAGCATAC	For constructing pYK006 plasmid. Template: pCMV_lox2272_loxp_inverse-*mvenus*_lox2272_loxp.
YKp0027	CATTAAAGAGGAGAAAGGTACCATAACTTCGTATAGGATAC	
YKp0029	CTTATTAGAATTCGCCGCCATGGTGAGCAAGGGCGAG	For constructing pYK007 plasmid using ExoIII cloning. PCR was conducted on the template pTmCherryK3 with YKp0029 & YKp0030 and pYK006 with YKp0031 & YKp0032 to convert *mvenus* to *mcherry*.
YKp0030	CATTATACGAAGTTATCTCGAGTTATCCACGCGTGAGC	
YKp0031	CTCGAGATAACTTCGTATAATG	
YKp0032	GGCGGCGAATTCTAATAAGG	

YKp0035	ATAACTTCGTATAAAGTATCCTATACGA AGTTATGGTACC	For constructing pYK008 plasmid. PCR was conducted on the template pYK007 to delete spacer sequence.
YKp0036	ATGGTGAGCAAGGGCGAGGAGGATAA CATGGCCATCATC	
YKp0037	TAACTCGAGATAACTTCGTATAATG	For constructing pYK009 plasmid with the template pYK008 to delete SacI and MluI restriction sites.
YKp0038	CTTGTACAGCTCGTCCATGC	
YKp0039	GAAAAAAATAACTTCGTATAGGATAC	For constructing pYK010 plasmid with the template pYK009 to change the ribosomal binding site (RBS).
YKp0040	CTCCTCTTTAATGTTTTCGGTCAGTGCG	
YKp0041	GAAGTTATAGGAGGAAAAAAATGGTGA GCAAGGGCGAGGAGG	For constructing pYK011 plasmid with the template pYK010 to transfer RBS in floxed site.
YKp0042	GTATAAAGTATCCTATACGAAGTTATCT TTAATGTTTTCGGTCAGTGCG	
YKp0069	CCGAAAACATTAAAGATAACTTCGTATA GCATACATTATACG	For constructing pYK023 with the template pYK011 (YKp0041 & YKp0069) to change lox2272 to loxP.
YKp0083	ATACATTATACGAAGTTATCAGGCATCA AATAAAACG	For constructing pYK028 plasmid with the template pYK023 to change the direction of loxP site.
YKp0084	GCTATACGAAGTTATCTCGAGTTACTTG TACAGCTC	
YKp0072	CGAGCTGTACAAGGAGCTCGAGAAAAA AATCACTGG	For constructing pYK029 plasmid using ExoIII cloning. PCR was conducted on the template pYK028 (YKp0072 YKp0089) and pTVCK4 (YKp0075 & YKp0083) to insert *cat* gene.
YKp0075	CTTGTACAGCTCGTCCATGCCGCCGGT GG	
YKp0089	CGTATAATGTATGCTATACGAAGTTATCT CGAGTTATCCAC	
YKp0109	GAGAAAAAAATCACTGG	For constructing pYK035 plasmid with the template pYK029 to remove *mcherry* gene.
YKp0110	CATTTTTTTCCTCCTATAAC	

Genome integration by λ-Red recombination

Name	Sequence	Usage
intC_Ptet O1_F3	AGTTGTTAAGGTCGCTCACTCCACCTTC TCATCAAGCCAGTCCGCCCATCCCTAT CAGTGATAGAGATTG	For genome integration of floxed *mcherry-cat*-FRT-*kan*-FRT or *cat*-FRT-*kan*-FRT at *intC* site by λ-Red recombination. PCR was conducted on the template pYK029 or pYK035.
intC_R	CCGTAGATTTACAGTTCGTCATGGTTCG CTTCAGATCGTTGACAGCCGCAATTCC GGGGATCCGTCGACC	
oMU94	ACCTGCGTGAGCGTACTGGTAAGGCTGC TCGTATCAAAGAGCGTCTTAACGTGAG CAAGGGCGAGGA	For integrating *mcherry*-FRT-*kan*-FRT fragment at *rplS* site. Template: pMU1.
oMU107	GCCAGCCAATTGGCCAGCCCTTCTTAAC AGGATGTCGCTTAAGCGAAATCTTGTG TAGGCTGGAGCTGCT	
oMU92	GTTCTCAGGATCTGGCTTCCCAGGCGG AAGAAAGCTTCGTAGAAGCTGAGGTG AGCAAGGGCGAGGA	For integrating *mvenus*-FRT-*kan*-FRT fragment at *rpsB* site. Template: pMU2.
oMU108	TTGCCGCCTTTCTGCAACTCGAACTATT TTGGGGGAGTTATCAAGCCTTATTGTG TAGGCTGGAGCTGCT	

Primers for sequence check

| Name	Sequence	Usage
M13F	CAGGAAACAGCTATGAC	Sequence check for the pMW118 derivative plasmids.
pM1_pVT_ seq_primer1	GGCACCCCAGGCTTTAC	
intC_ check_F	GATCGATACTTGCTGTGGTTGATG	Sequence check for the *intC* site.
intC_ check_R2	CCTCTTAGTTAAATGGATATAACGAGCC CC	
YKp0077	CACCGTTGATATATCCCAATGGC	Sequence check for the *cat* gene.
YKp0115	CACTCATCGCAGTACTGTTG	
oMU96	TCCAGACTCACTCTCCGGTAGT	Sequence check for the *rplS* site. For the BW25113 derivative strains oMU96 & oMU97; For the W3110 derivative strains oMU96 & oMU110
oMU97	ATAGCCAGTAACAAGACCGCCC	
oMU110	GACAAATTCCACGCAGCAATCTCAC	
oMU26	AAGCAAACAACCTGGGTATTCCGGT	Sequence check for the *rpsB* site
oMU28	CTCGCTCATCCCGGTCACTTACTGA	

Supplemental Figures

518
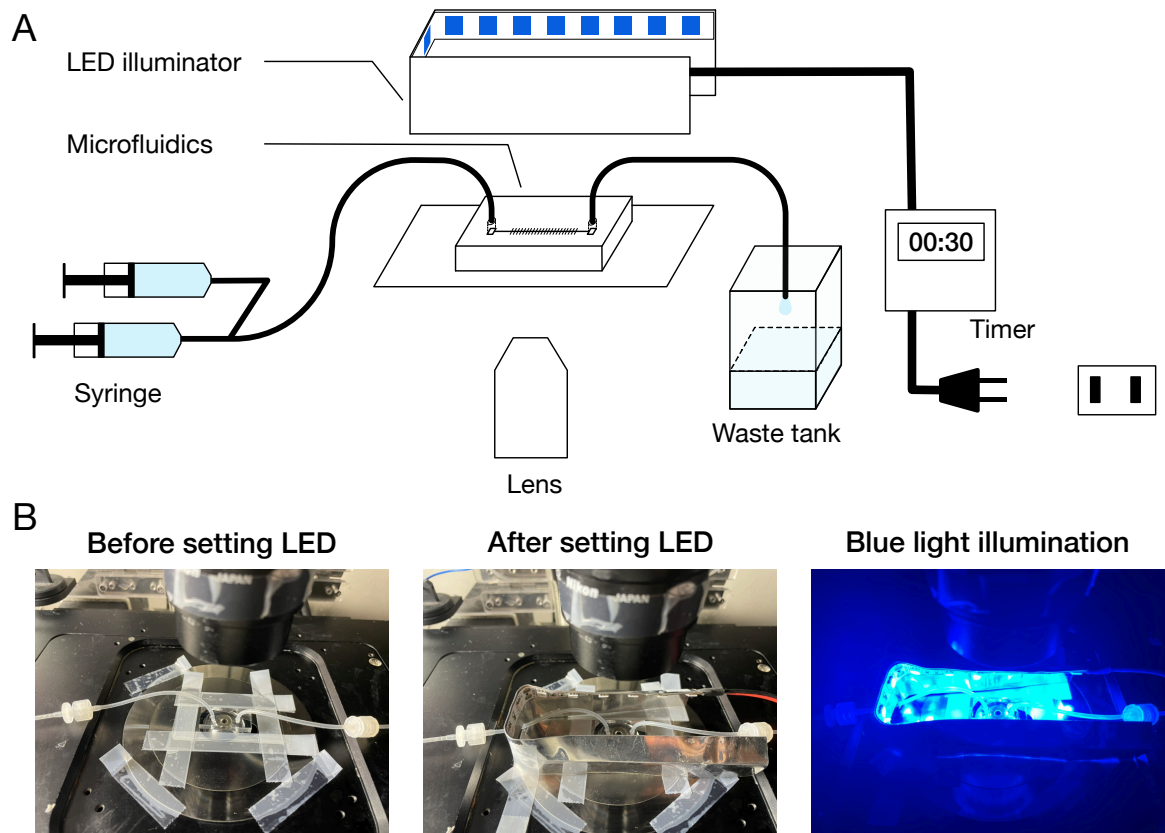
Figure S1. On-stage blue-light LED illuminator. (A) Schematic diagram of microscope setup. A custom blue-light LED illuminator was placed on the microscope stage to illuminate the microfluidic device. The timing and duration of illumination were controlled by an external timer. (B) Photo images of the microfluidic device and LED illuminator mounted on the microscope stage.
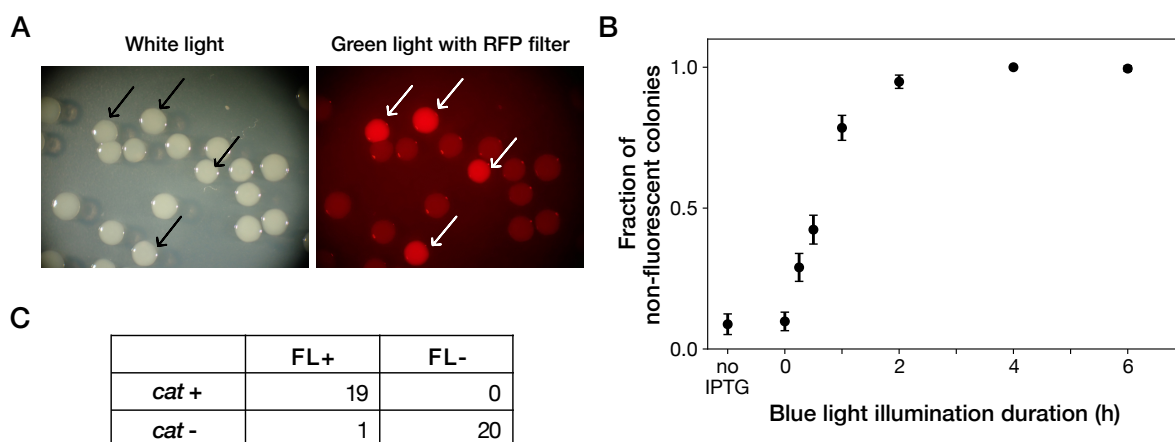
A

White light   Green light with RFP filter

B

C

	FL+	FL-
cat +	19	0
cat -	1	20

Figure S2. Resistance gene deletion by blue-light illumination in batch cultures. (A) Colonies of YK0083 cells inoculated after blue-light illumination. The YK0083 cells were exposed to blue light for 1 h in batch culture and spread on agar. The colonies were photographed under the exposure of ambient light (left) and excitation light (right). The colonies of the cells retaining the *mcherry-cat* gene were visually detectable under the excitation light (arrows). (B) Relationship between blue-light illumination duration and fractions of non-fluorescent colonies. Black points represent the means. Error bars represent standard errors ($N = 239$ for no IPTG; $N = 327$ for 0 h; $N = 335$ for 0.25 h; $N = 373$ for 0.5 h; $N = 344$ for 1 h; $N = 350$ for 2 h; $N = 296$ for 4 h; $N = 209$ for 6 h). "no IPTG" represents the condition where the cells were cultured in the M9 medium without IPTG and not exposed to blue light. (C) The correspondence between mCherry-CAT fluorescence and presence of the *cat* resistance gene. FL+ and FL- represent the presence/absence of mCherry fluorescence visually inspected for the colonies. *cat+* and *cat-* represent the presence/absence of the *cat* gene detected by colony PCR. All non-fluorescent colonies had lost the *cat* gene. All but one fluorescent colony retained the *cat* gene.
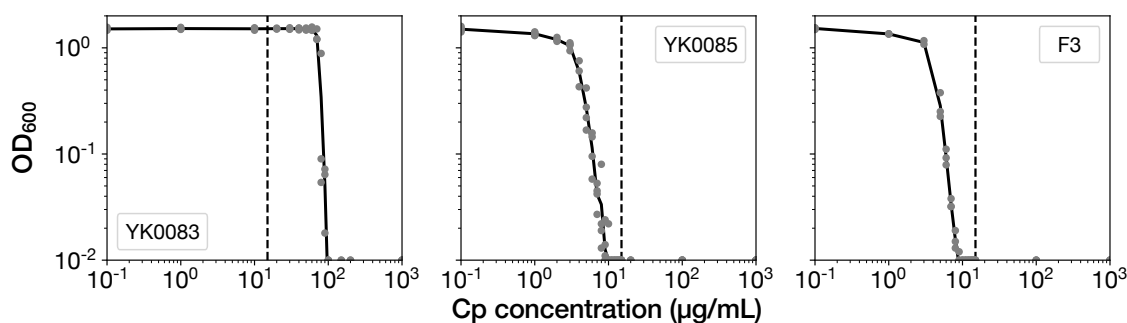

Figure S3. MIC tests. Gray points represent the OD_{600} of the indicated strains after a 23 h incubation period in the M9 media containing the corresponding concentrations of Cp. The minimum concentration where OD_{600} became lower than 0.01 was adopted as the MIC for each strain. 15 μg/mL of Cp was used in the time-lapse experiments (dashed line). The measurements were repeated at least thrice.
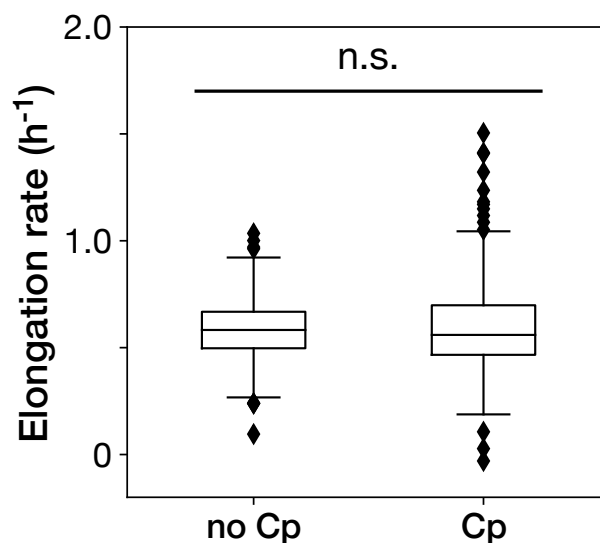
Figure S4. The Cp concentration used in the time-lapse measurements caused no significant effect on the growth of non-deleted YK0083 cells. Box plots show the elongation rates of the YK0083 cells growing in the mother machine. "no Cp" denotes the drug-free condition; "Cp" denotes the condition under the exposure of 15 μg/mL of Cp. The elongation rates were obtained from the non-deleted cell lineages up to ten generations after blue-light illumination. We detected no significant differences in elongation rates between the two conditions ($p = 0.63$, Welch's t-test).
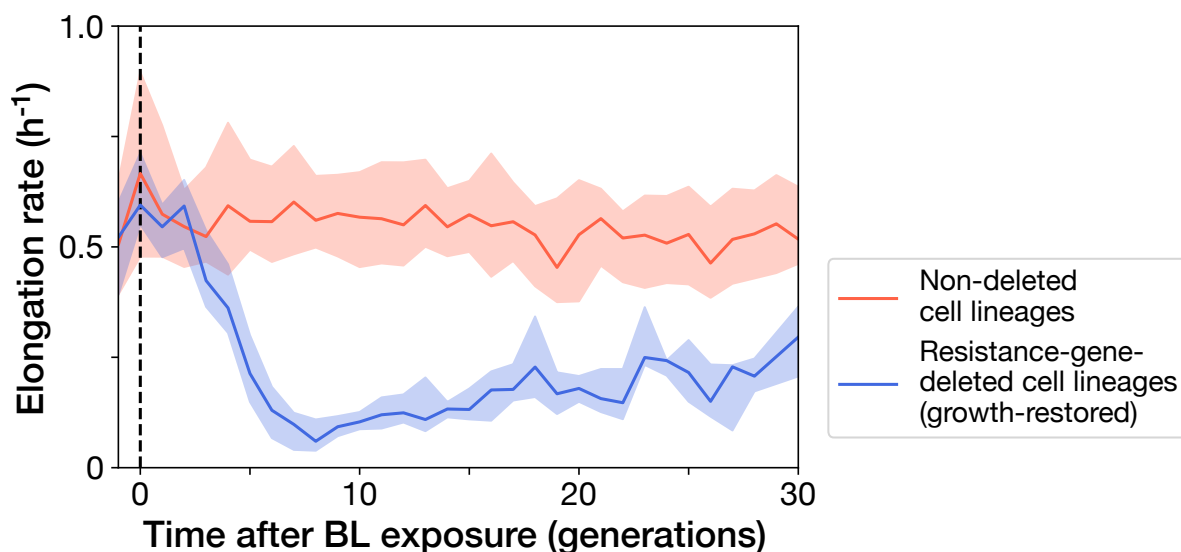
Figure S5. Transitions of elongation rates after blue-light illumination. The YK0083 cells were exposed to blue light for 30 min from $t = $ -0.5 h to 0 h. The lines and shaded areas represent the medians and the 25-75% data ranges, respectively. Red represents the non-deleted cell lineages. Blue represents the growth-restored resistance-gene-deleted cell lineages.
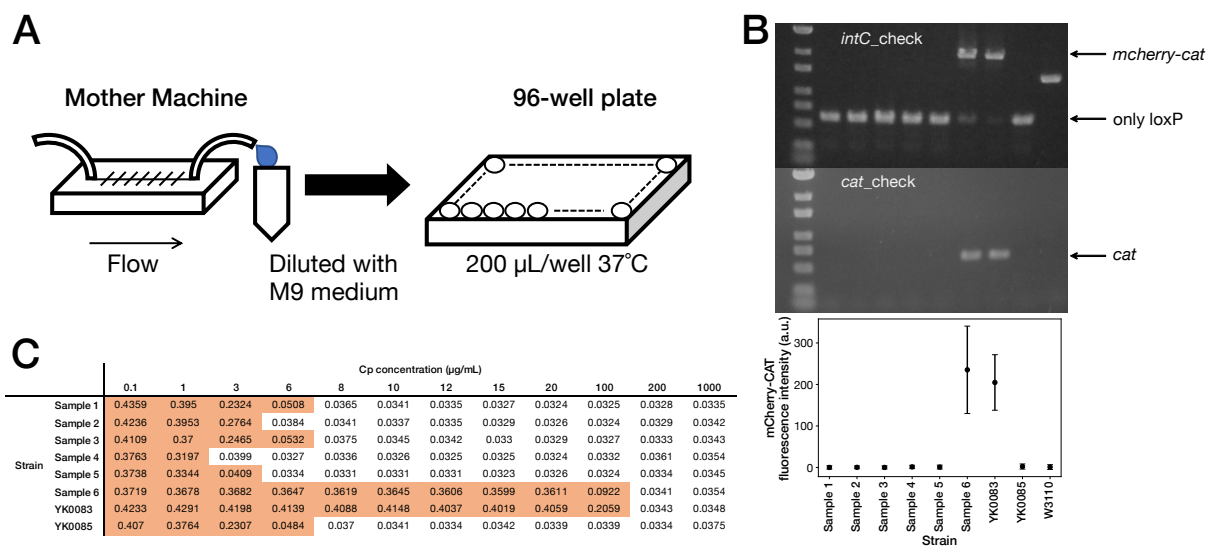
A

B

C

Strain	Cp concentration (µg/mL)											
	0.1	1	3	6	8	10	12	15	20	100	200	1000
Sample 1	0.4359	0.395	0.2324	0.0508	0.0365	0.0341	0.0335	0.0327	0.0324	0.0325	0.0328	0.0335
Sample 2	0.4236	0.3953	0.2764	0.0384	0.0341	0.0337	0.0335	0.0329	0.0326	0.0324	0.0329	0.0342
Sample 3	0.4109	0.37	0.2465	0.0532	0.0375	0.0345	0.0342	0.033	0.0329	0.0327	0.0333	0.0343
Sample 4	0.3763	0.3197	0.0399	0.0327	0.0336	0.0326	0.0325	0.0325	0.0324	0.0332	0.0361	0.0354
Sample 5	0.3738	0.3344	0.0409	0.0334	0.0331	0.0331	0.0331	0.0323	0.0326	0.0324	0.0334	0.0345
Sample 6	0.3719	0.3678	0.3682	0.3647	0.3619	0.3645	0.3606	0.3599	0.3611	0.0922	0.0341	0.0354
YK0083	0.4233	0.4291	0.4198	0.4139	0.4088	0.4148	0.4037	0.4019	0.4059	0.2059	0.0343	0.0348
YK0085	0.407	0.3764	0.2307	0.0484	0.037	0.0341	0.0334	0.0342	0.0339	0.0339	0.0334	0.0375

Figure S6. Correspondence between fluorescence loss and *mcherry-cat* gene deletion in the cells sampled from the mother machine. (A) The scheme for acquiring the resistance-gene-deleted cells from the mother machine. The culture media flowing out from the mother machine were sampled to obtain the cells that lost the *mcherry-cat* gene. The media were diluted serially, and the limited-diluted media were taken in 96-well plates and incubated. (B) Correspondence between fluorescence loss and gene deletion. The cell populations were collected from the 96-well plates, and the deletion of *mcherry-cat* gene was examined by PCR. We detected no bands of both *mcherry-cat* and *cat* for Samples 1-5. Sample 6 retained the *mcherry-cat* gene. The bottom plot shows that the absence of *mcherry-cat* gene corresponds to the loss of mCherry-CAT fluorescence. (C) MIC test. The OD_{600} values of Samples 1-6, YK0083 and YK0085 after a 23 h incubation period at the indicated Cp concentrations are shown (Start OD_{600}, 0.001). The entries with colored backgrounds indicate $OD_{600} > 0.04$.
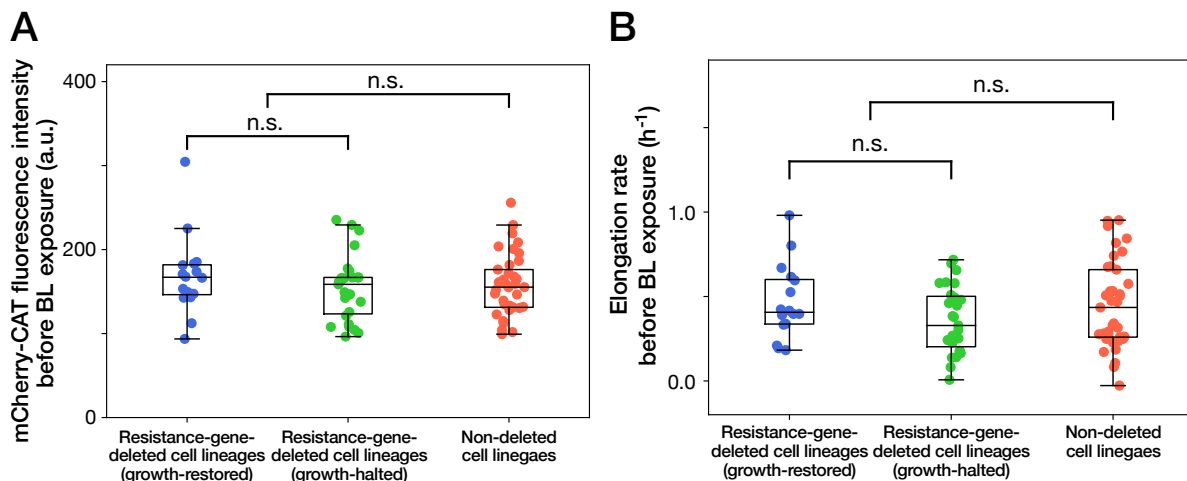
Figure S7. Cellular phenotypes before blue-light illumination do not correlate with the cellular fates. (A) mCherry-CAT fluorescence before blue-light illumination. Each point represents the fluorescence intensity of single-cell lineage averaged over the 1 h period immediately before blue-light illumination. Blue points represent the growth-restored resistance-gene-deleted cell lineages. Green points represent the growth-halted resistance-gene-deleted cell lineages. Red points represent the non-deleted cell lineages. $p = 0.30$ for growth-restored resistance-gene-deleted cell lineages vs growth-halted resistance-gene-deleted cell lineages; $p = 0.85$ for resistance-gene-deleted cell lineages vs non-deleted cell lineages, Welch's t-test. (B) Elongation rates before blue-light illumination. Each point represents the elongation rate of single-cell lineage averaged over the 1 h period immediately before blue-light illumination. The color correspondence remains the same as A. $p = 0.12$ for growth-restored resistance-gene-deleted cell lineages vs growth-halted resistance-gene-deleted cell lineages; $p = 0.35$ for resistance-gene-deleted cell lineages vs non-deleted cell lineages, Welch's t-test.
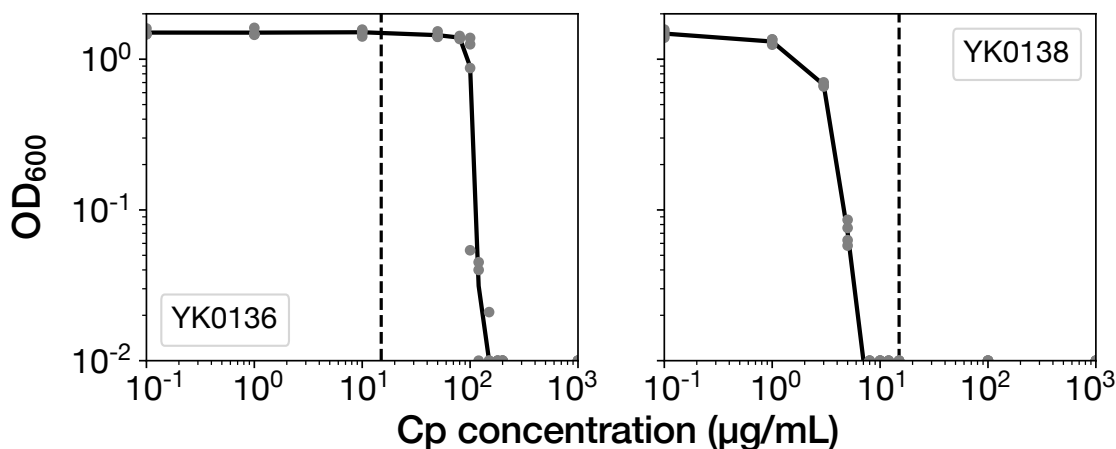
Figure S8. MIC tests of the ribosome reporter strains. Gray points indicate the OD_{600} of the cell cultures after a 23 h incubation period in the media containing the corresponding concentrations of Cp. The left shows the result of YK0136. The right shows the result of YK0138. The minimum concentration where OD_{600} became lower than 0.01 was adopted as the MIC for each strain. 15 μg/mL of Cp was used in the experiments (dashed line). The measurements were repeated at least thrice.
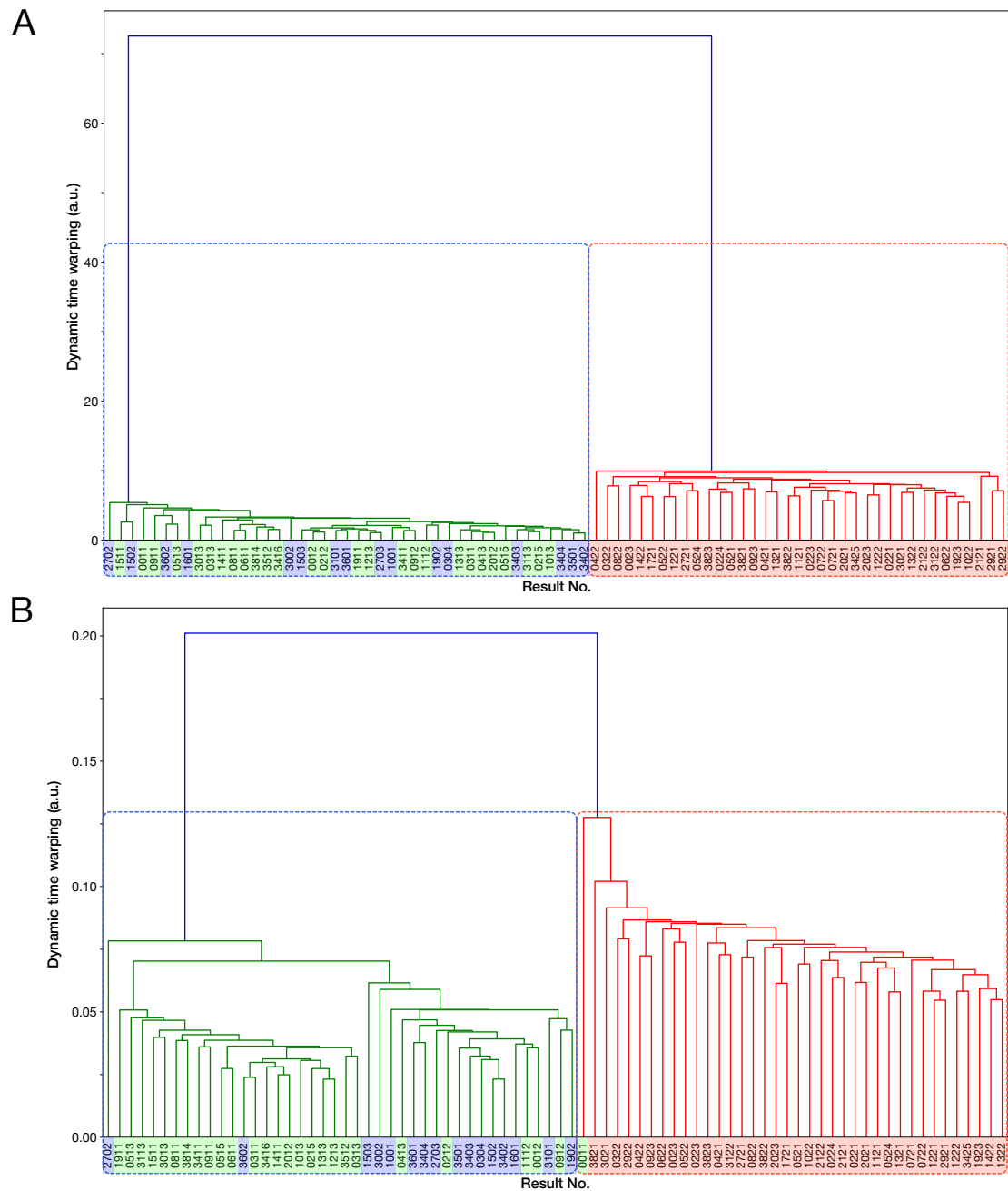
Figure S9. Time-course transitions of elongation rates are sufficient for classifying resistance-gene-deleted and non-deleted cell lineages. (A) Hierarchical clustering of single-cell lineages based on the transitions of mCherry-CAT fluorescence intensities. The mCherry-CAT fluorescence transitions in single-cell lineages over the entire periods of measurement were used for clustering. The distances between cell lineages were calculated by dynamic time warping. The numbers shown on the horizontal axis represent cell lineage IDs. The background colors behind the cell lineage IDs represent the fates of cell lineages assigned manually by the experimenters: Blue corresponds to growth-restored resistance-gene-deleted cell lineages; Green represents growth-halted resistance-gene-deleted cell lineages; Red represents non-deleted cell lineages. (B) Hierarchical clustering of single-cell lineages based on the transitions of elongation rates. The cell lineage clusters indicated by the blue and red dotted lines constitute two main groups, corresponding to resistance-gene-deleted and non-deleted cell lineages, respectively. Only one resistance-gene-deleted cell lineage (0011) was assigned wrongly as a non-deleted cell lineage. Therefore, the transitions of elongation rates are sufficient for classifying the resistance-gene-deleted and non-deleted cell lineages at high precision.
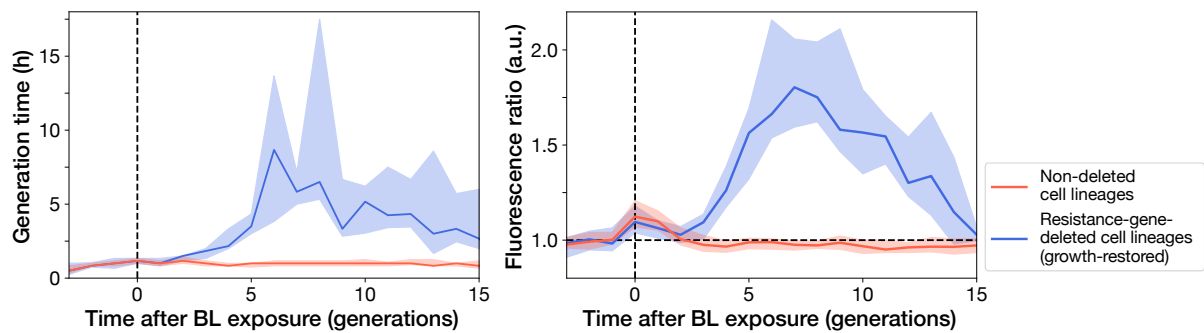
Figure S10.   Transitions of generation time and RplS-mCherry/RpsB-mVenus fluorescence ratio observed in ribosome reporter strain shown in the time unit of generation. Left: Generation time transitions; Right: RplS-mCherry/RpsB-mVenus fluorescence ratio transitions. The lines and shaded areas represent the medians and the 25-75% data ranges, respectively. Blue corresponds to growth-restored resistance-gene-deleted cell lineages. Red corresponds to non-deleted cell lineages.
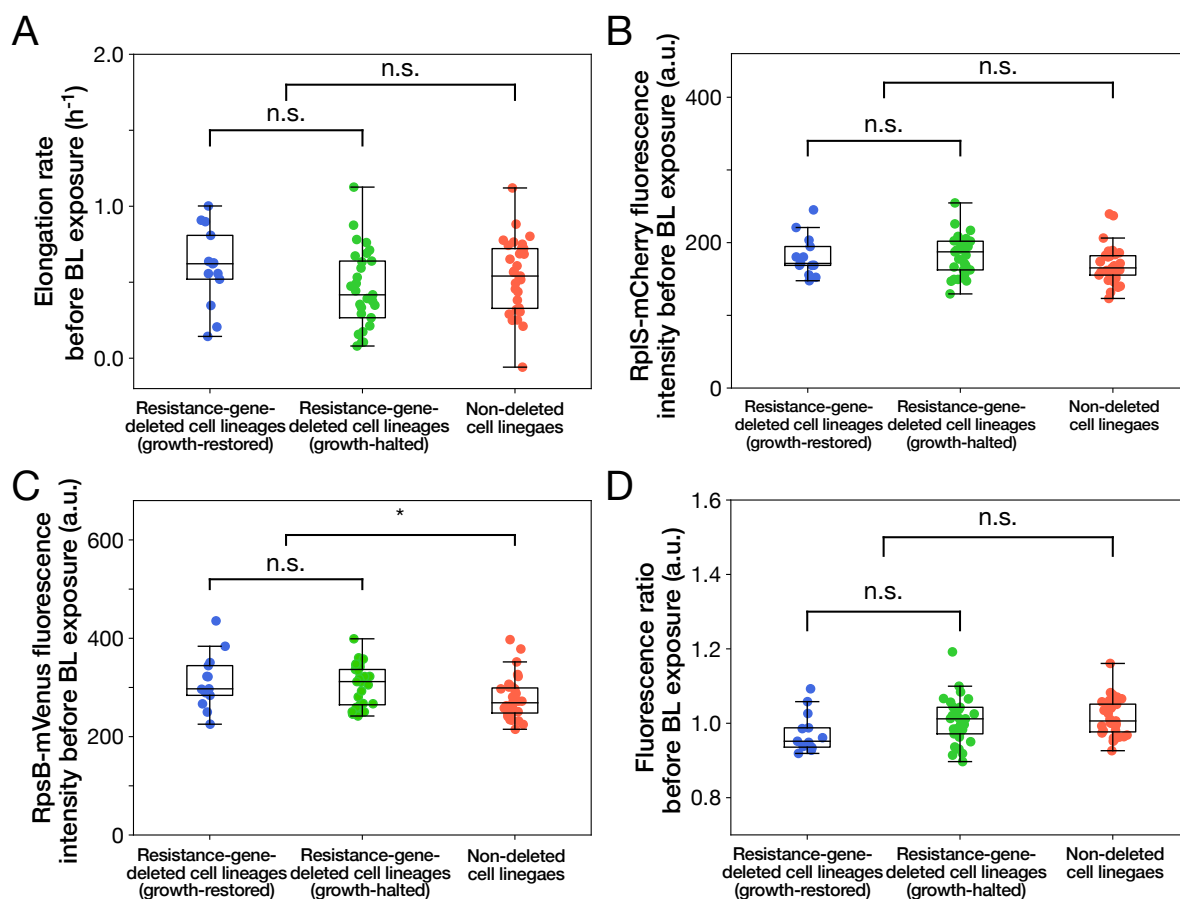
Figure S11. Relationships between cellular phenotypes before blue-light illumination and cellular fates. (A) Relationship between elongation rates before blue-light illumination and cellular fates. Blue represents growth-restored resistance-gene-deleted cell lineages. Green represents growth-halted resistance-gene-deleted cell lineages. Red represents non-deleted cell lineages (Color correspondence remains the same in the following figures). Each point represents the elongation rate of single-cell lineage averaged over the 1 h period immediately before blue-light illumination. $p = 0.10$ for growth-restored vs growth-halted cell lineages; $p = 0.54$ for resistance-gene-deleted vs non-deleted cell lineages, Welch's t-test. (B) Relationship between RplS-mCherry fluorescence intensities averaged over the 1 h period before blue-light illumination and cellular fates. $p = 0.87$ for growth-restored vs growth-halted cell lineages; $p = 0.038$ for resistance-gene-deleted vs non-deleted cell lineages, Welch's t-test. (C) Relationship between RpsB-mVenus fluorescence intensities averaged over the 1 h period before blue-light illumination and cellular fates. $p = 0.60$ for growth-restored vs growth-halted cell lineages; $p = 0.010$ for resistance-gene-deleted vs non-deleted cell lineages, Welch's t-test. Asterisk denotes the statistical difference judged at the significance level of 0.01. (D) Relationship between RplS-mCherry/RpsB-mVenus fluorescence ratio averaged over the 1 h period before blue-light illumination and cellular fates. $p = 0.098$ for growth-restored vs growth-halted cell lineages; $p = 0.15$ for resistance-gene-deleted vs non-deleted cell lineages, Welch's t-test.